

อุณหภูมิกการเปลี่ยนแบบ BCC-HCP ของโลหะไทเทเนียม โดยใช้วิธีพลศาสตร์เชิงโมเลกุลแบบฉบับ



นายเจษฎา จุรีมาศ

สถาบันวิทยบริการ

วิทยานิพนธ์นี้เป็นส่วนหนึ่งของการศึกษาตามหลักสูตรปริญญาวิทยาศาสตรมหาบัณฑิต

สาขาวิชาฟิสิกส์ ภาควิชาฟิสิกส์

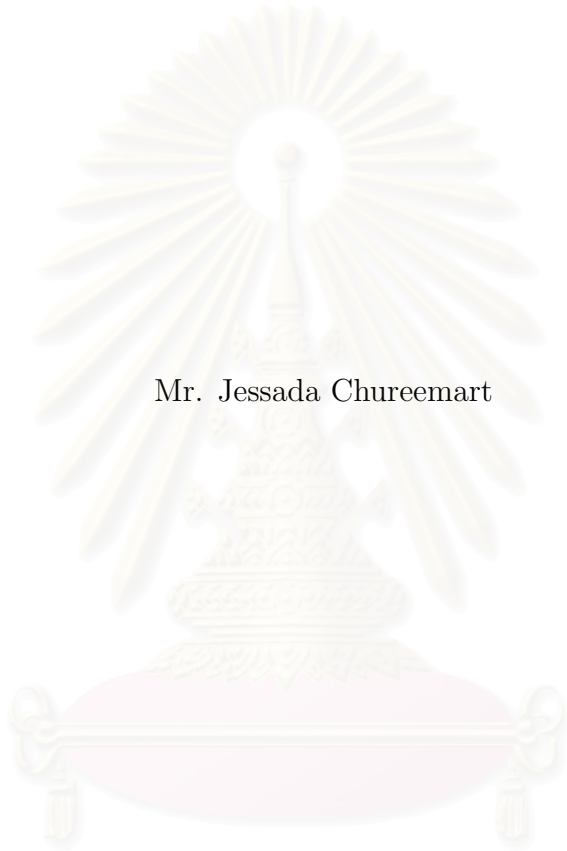
คณะวิทยาศาสตร์ จุฬาลงกรณ์มหาวิทยาลัย

ปีการศึกษา 2548

ISBN 974-17-4558-3

ลิขสิทธิ์ของจุฬาลงกรณ์มหาวิทยาลัย

THE BCC-HCP TRANSITION TEMPERATURE IN TITANIUM METAL  
USING THE CLASSICAL MOLECULAR DYNAMICS METHOD



Mr. Jessada Chureemart

A Thesis Submitted in Partial Fulfillment of the Requirements  
for the Degree of Master of Science Program in Physics

Department of Physics

Faculty of Science

Chulalongkorn University

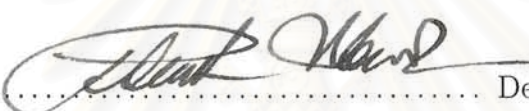
Academic year 2005

ISBN 974-17-4558-3

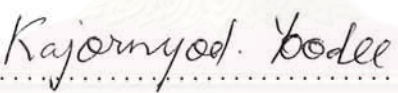
Thesis Title THE BCC-HCP TRANSITION TEMPERATURE IN TITANIUM METAL USING THE CLASSICAL MOLECULAR DYNAMICS METHOD  
By Mr. Jessada Chureemart  
Field of Study Physics  
Thesis Advisor Assistant Professor Udomsilp Pinsook, Ph.D.

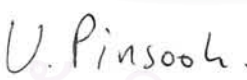
---


Accepted by the Faculty of Science, Chulalongkorn University in Partial Fulfillment of the Requirements for the Master's Degree


  
..... Dean of the Faculty of Science  
(Professor Piamsak Menasveta, Ph.D.)

#### THESIS COMMITTEE

  
..... Chairman  
(Assistant Professor Kajornyod Yodee, Ph.D.)

  
..... Thesis Advisor  
(Assistant Professor Udomsilp Pinsook, Ph.D.)

  
..... Member  
(Assistant Professor Chaising Poo-Rakkiat, Ph.D.)

  
..... Member  
(Assistant Professor Patcha Chatraphorn, Ph.D.)

เจษฎา จูรีมาศ : อุณหภูมิการเปลี่ยนแบบ BCC-HCP ของโลหะไทเทเนียมโดยใช้วิธีพลศาสตร์เชิงโมเลกุลแบบฉบับ. (THE BCC-HCP TRANSITION TEMPERATURE IN TITANIUM METAL USING THE CLASSICAL MOLECULAR DYNAMICS METHOD) อ. ที่ปรึกษา : ผศ.ดร. อุดมศิลป์ ปิ่นสุข, 70 หน้า. ISBN 974-17-4558-3.

ได้ใช้วิธีพลศาสตร์เชิงโมเลกุลมาคำนวณองค์ประกอบของพลังงานอิสระเฮล์มโฮลทซ์ของไทเทเนียมแบบ hcp และ bcc ที่อุณหภูมิตั้งแต่ 300 เคลวิน ถึง 1,300 เคลวิน ผลต่างของพลังงานภายในจะถูกคำนวณจากผลต่างของพลังงานศักย์ ได้เลือกพลังงานศักย์แบบฟินนิส-ซินแคลร์ (Finnis-Sinclair) มาใช้แทนพลังงานศักย์ของไทเทเนียม ส่วนเอนโทรปีรวมประกอบด้วยอิเล็กตรอนิกเอนโทรปีและเอนโทรปีจากการสั่นซึ่งรวมเอนโทรปีจากการสั่นของฮาร์โมนิกส์และแอนฮาร์โมนิกส์ คำนวณอุณหภูมิการเปลี่ยนสถานะได้มีค่าเท่ากับ 880 เคลวิน ที่ซึ่งปริมาณผลต่างของพลังงานอิสระเฮล์มโฮลทซ์ระหว่างสองสถานะมีค่าเท่ากับศูนย์ ผลการศึกษานี้สอดคล้องกับค่าที่วัดได้จากการทดลอง



สถาบันวิทยบริการ  
จุฬาลงกรณ์มหาวิทยาลัย

ภาควิชาฟิสิกส์.....ลายมือชื่อนิสิต..... Jessada Chuseemast  
สาขาวิชาฟิสิกส์.....ลายมือชื่ออาจารย์ที่ปรึกษา..... U. P. 175066  
ปีการศึกษา 2548.....

## 4572263123 :MAJOR PHYSICS

KEY WORDS: TRANSITION TEMPERATURE / HELMHOLTZ FREE ENERGY / HARMONIC VIBRATION ENTROPY / ANHARMONIC VIBRATION ENTROPY / ELECTRONIC ENTROPY

JESSADA CHUREEMART : THE BCC-HCP TRANSITION TEMPERATURE IN TITANIUM METAL USING THE CLASSICAL MOLECULAR DYNAMICS METHOD. THESIS ADVISOR : ASST. PROF. UDOMSILP PINSOOK, PH.D., 70 pp. ISBN 974-17-4558-3.

Molecular dynamics is carried out in order to calculate the component of Helmholtz free energy of the hcp and the bcc titanium at temperature from 300K to 1,300K. The internal energy difference is calculated from the potential energy difference. The Finnis-Sinclair potential energy is chosen to represent the potential energy of titanium. The total entropy consists of the electronic entropy and the vibrational entropy including harmonic and anharmonic vibrational entropy. The transition temperature is identified at 880K where Helmholtz free energy difference between the two phases is equal to zero. This finding is in agreement with experiments.

สถาบันวิทยบริการ  
จุฬาลงกรณ์มหาวิทยาลัย

Department Physics..... Student's signature .. Jessada Chureemart ..

Field of study Physics..... Advisor's signature .. U. Pinsook ..

Academic year 2005 .....



# ACKNOWLEDGEMENTS

My thesis has been done under the supervision of Assistant Professor Dr. Udomsilp Pinsook. I would like to express my sincere gratitude and appreciation to my advisor, for guidance, suggestion, support throughout this thesis, and opportunity to work in his research group. I wish to thank Dr. Chatchai Srinitiwarawong and Mr. Pornjuk Srepusharawoot for advice and assistance during the period of my graduate studies.

I am grateful to the chairman, Assistant Professor Kajornyod Yoodee, the committee, Assistant Professor Chaisingh Poo-Rakkiat, and Assistant Professor Patcha Chatraphorn. I would like to acknowledge the financial support by the Development and Promotion for Science and Technology Talents Project of Thailand (DPST).

I would like to say thanks to my friends and colleagues, who have been helpful. Lastly, I would like to express gratitude to my family for their love, understanding, support and encouragement.

สถาบันวิทยบริการ  
จุฬาลงกรณ์มหาวิทยาลัย

# TABLE OF CONTENTS

Abstract (Thai) .....	iv
Abstract (English).....	v
Acknowledgements .....	vi
List of Figures.....	xi
List of Tables.....	xii
<b>Chapter</b>	
<b>I Introduction.....</b>	<b>1</b>
<b>II Molecular Dynamics Method .....</b>	<b>8</b>
2.1 General Description of The MD Method .....	8
2.1.1 Gear Predictor-Corrector method .....	10
2.1.2 Choice of a time step .....	13
2.2 The Potential Energy for Titanium .....	14
2.3 The Kinetic Energy .....	20
2.4 Measuring The Pressure .....	22

<b>III The Total Entropy</b> .....	<b>25</b>
3.1 Harmonic Vibrational Entropy . . . . .	25
3.1.1 Phonon density of states in the bcc and hcp phases . . . . .	30
3.2 Anharmonic Vibrational Entropy . . . . .	32
3.3 Electronic Entropy . . . . .	34
<b>IV Results And Discussion</b> .....	<b>39</b>
4.1 The True Lattice Constant . . . . .	41
4.2 The Internal Energy Difference . . . . .	44
4.3 The Phonon Density of States . . . . .	48
4.4 The Vibrational Entropy . . . . .	52
4.5 The Electronic Entropy . . . . .	58
4.6 The Transition Temperature . . . . .	61
<b>V Conclusions</b> .....	<b>63</b>
<b>References</b> .....	<b>66</b>
<b>Vitae</b> .....	<b>70</b>

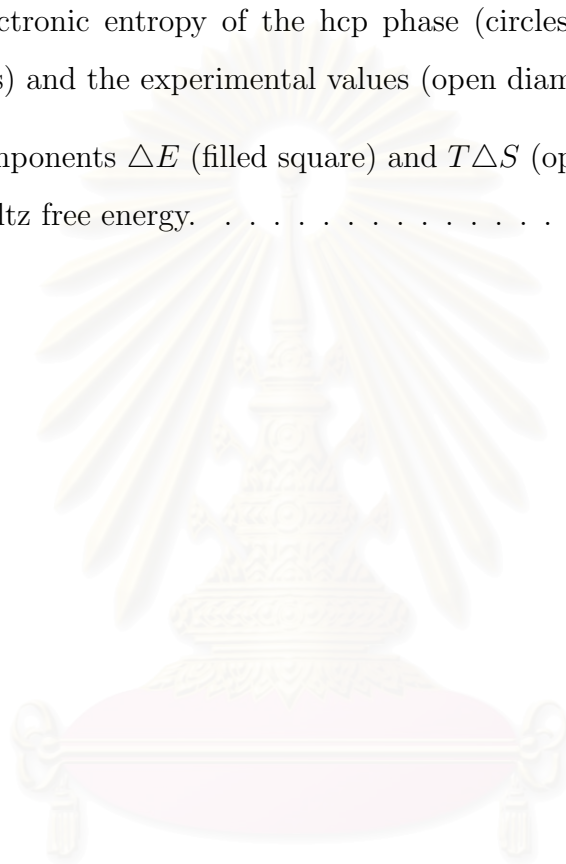


# LIST OF FIGURES

1.1	P-T Phase diagram of titanium [1] . . . . .	2
1.2	The body centered cubic structure . . . . .	3
1.3	The atomic positions in the body centered-cubic at $(110)_{\text{bcc}}$ . . . . .	3
1.4	Illustrate the transformation from bcc to hcp . . . . .	4
1.5	The atomic positions in the hexagonal close-packed in $(0001)_{\text{hcp}}$ . . . . .	4
1.6	The hexagonal close-packed structure . . . . .	5
2.1	Flow chart of the MD simulation . . . . .	11
2.2	The potential energy of the hcp phase at 1,200K . . . . .	17
2.3	The potential energy of the bcc phase at 900K . . . . .	18
2.4	Typical of the potential energy curve . . . . .	19
2.5	a) the pressure of the hcp phase from the <b>MD</b> simulation at 500K and lattice constant = 2.95Å. b) the pressure-lattice constant rela- tionship of the hcp phase at 500K . . . . .	24
3.1	a) The velocity autocorrelation $\gamma(t)$ taken from the hcp phase with 6,912 atoms at 1,000 K, b) the phonon density of states in the hcp phase from the fourier transform of $\gamma(t)$ . . . . .	32
3.2	Electronic density of states for the hcp structures of Ti.[3] . . . . .	37
3.3	Electronic density of states for the bcc structures of Ti.[3] . . . . .	38

4.1	The pressure of the bcc phase for $a=3.2\text{\AA}$ , $3.25\text{\AA}$ , $3.278\text{\AA}$ , $3.28\text{\AA}$ and $3.3\text{\AA}$ at $T=1, 100K$ . . . . .	42
4.2	The lattice constant of the hcp phase with $P=0$ at constant temperatures: $T = 300K, 400K, 500K, 600K, 700K, 800K, 900K, 1,000K, 1,100K, 1,200K$ , and $1,300K$ . . . . .	43
4.3	The lattice constant of the bcc phase with $P=0$ at constant temperatures: $T = 300K, 400K, 500K, 600K, 700K, 800K, 900K, 1,000K, 1,100K, 1,200K$ , and $1,300K$ . . . . .	44
4.4	The potential energy of the hcp (open circles) and the bcc (filled squares) phases as a function of temperature. . . . .	46
4.5	Velocity autocorrelation function of the hcp phase at $300K, 400K$ and $500K$ , going from bottom to top . . . . .	49
4.6	Velocity autocorrelation function of the bcc phase at $1000K, 1100K$ and $1200K$ , going from bottom to top . . . . .	50
4.7	The phonon density of states of the hcp phase at $1,000K$ . . . . .	51
4.8	The phonon density of states of the bcc phase at $1,000K$ . . . . .	52
4.9	The calculated values of the harmonic vibrational entropy of the hcp (filled squares) and the bcc phases (open circles) . . . . .	53
4.10	The anharmonic contribution of the hcp (open circles) and the bcc (filled squares) structures. . . . .	54
4.11	The calculated values of the total vibrational entropy of the hcp Ti (filled squares) compared with the experimental values [4] (open circles). . . . .	57

4.12	The calculated values of the total vibrational entropy of the bcc Ti (filled squares) compared with the experimental values [4] (open circles). . . . .	58
4.13	The electronic entropy of the hcp phase (circles), the bcc phase (squares) and the experimental values (open diamonds)[9]. . . . .	59
4.14	The components $\Delta E$ (filled square) and $T\Delta S$ (open circles) of the Helmholtz free energy. . . . .	61



สถาบันวิทยบริการ  
จุฬาลงกรณ์มหาวิทยาลัย

# LIST OF TABLES

2.1	Fitting parameters $k$ , $A_k$ , $R_k$ , $a_k$ and $r$ for titanium [11] . . . . .	16
4.1	Numerical figures of the potential energy ( $E$ ) and the lattice constants ( $a$ ) of the hcp and the bcc phases. . . . .	47
4.2	Numerical figures of the harmonic vibrational entropy ( $S_H$ ) and the anharmonic vibrational entropy ( $S_A$ ) of the hcp and the bcc phases.	56
4.3	Numerical figures of the electronic entropy ( $S_E$ ) from MD method and experimental values [9]of the hcp and the bcc phases. . . . .	60



สถาบันวิทยบริการ  
จุฬาลงกรณ์มหาวิทยาลัย

# CHAPTER I

## INTRODUCTION

Titanium was discovered in 1791 by Gregor and it was named in 1795 by Klaproth. In 1910, the pure titanium metal was extracted by Hunter. Titanium is a transition metal in group IVB. It has many similarities to zirconium and hafnium because the three metals are in the same column or group in the periodic table. Titanium is a white silvery-metallic color, strong and lustrous metal. It has the symbol Ti, atomic number 22 and atomic mass 47.90 g/mol. The electronic configuration is  $[\text{Ar}]4s^23d^2$ . The shell structure is 2.8.10.2. Ti has a low density of 4,540 kg/m<sup>3</sup> which is lighter than steel but heavier than aluminum. It is as strong as steel. The melting point is 1,941 K which is higher than steel. Therefore, Ti is used extensively in aerospace structural application. Ti has a small coefficient of thermal expansion of  $8.4 \times 10^{-6} \text{K}^{-1}$  which is lower than steel and aluminum. It is a nonmagnetic material with permeability of 1.00005-1.00010. The thermal conductivity of titanium is relatively low for a metal. It is  $21.6 \text{ W}^{-1}\text{K}^{-1}$  which is lower than zirconium. Furthermore, the titanium metal has excellent resistance to sea water and is used for propeller shafts, rigging, and other parts of ships exposed to salt water.

Moreover, an important phenomenon of titanium is the martensitic phase transition. It is crystallographic phase change into a different crystal structure under high temperature and pressure. The martensitic phase transitions has 2

modes. The first,  $\alpha$ - $\beta$  **phase transition**, is a transformation from hexagonal close-packed structure ( $\alpha$ -phase) into body centered cubic ( $\beta$ -phase) by increasing temperature. Another mode,  $\alpha$ - $\omega$  **phase transition**, which is beyond the scope of our work, is a transformation from  $\alpha$ -phase into another close-packed structure ( $\omega$ -phase) at high pressure. The phase diagram of titanium is shown in Fig 1.1.

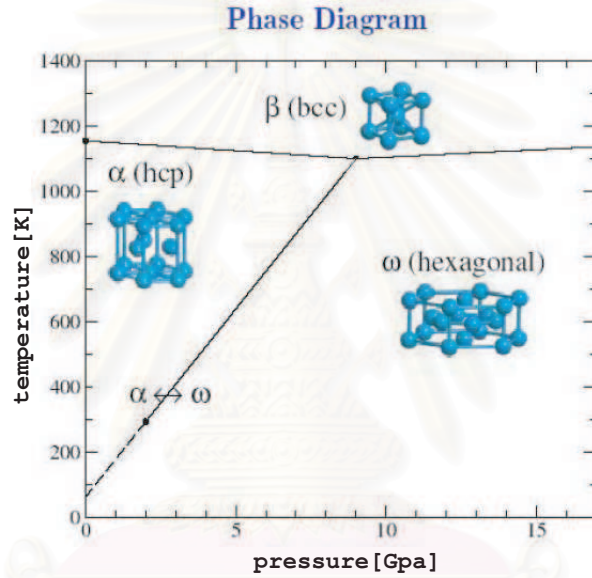


Figure 1.1: P-T Phase diagram of titanium [1]

To describe the path of the bcc to hcp phase transition, we consider **Burger's distortions**[2]. It is the simplest path of transformation from the bcc structure into the hcp structure. This transformation can be regarded as a distortion of the bcc lattice. The structure is shown in Fig 1.2. We consider bcc  $(110)_{\text{bcc}}$  plane which has  $109.5^\circ$  bond angle as in Fig 1.3. If the temperature is lower than transition temperature, then the bcc phase is transformed into the hcp phase of which the lattice constant is  $2.95 \text{ \AA}$  and  $c/a$  ratio of 1.588 [3].



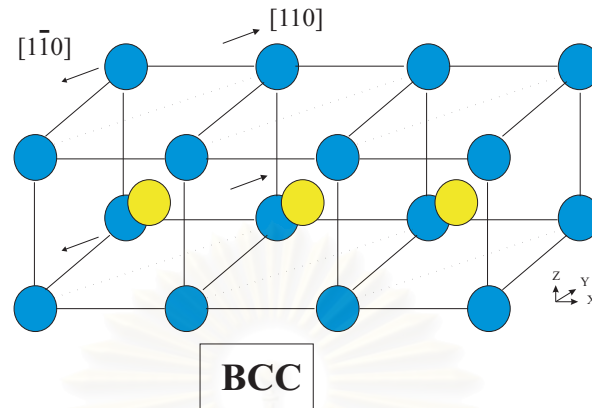


Figure 1.2: The body centered cubic structure

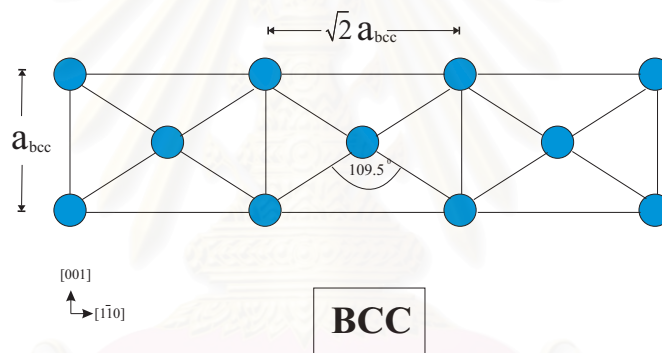


Figure 1.3: The atomic positions in the body centered-cubic at  $(110)_{bcc}$

This transformation can be considered as an orthorhombic distortion of  $(110)_{bcc}$ . The distance between atoms along  $[1\bar{1}0]$  are modified from  $\sqrt{2}a_{bcc}$  into  $\sqrt{3}a_{hcp}$  and the  $109.5^\circ$  bond angle changes to  $120^\circ$  in  $(110)_{bcc}$ . The path of transformation is shown in Fig 1.4 and Fig 1.5.

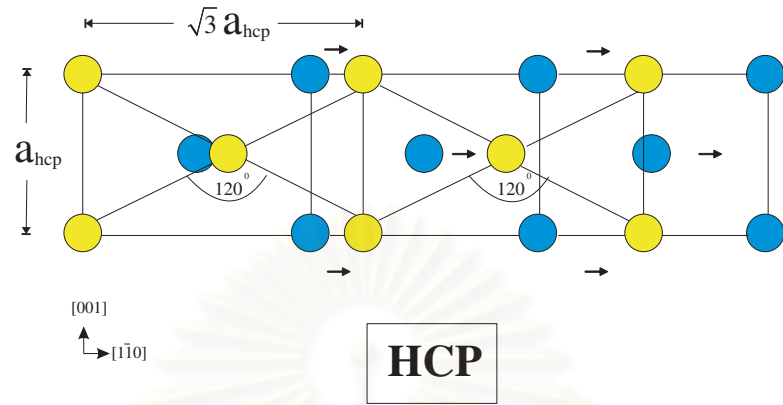


Figure 1.4: Illustrate the transformation from bcc to hcp

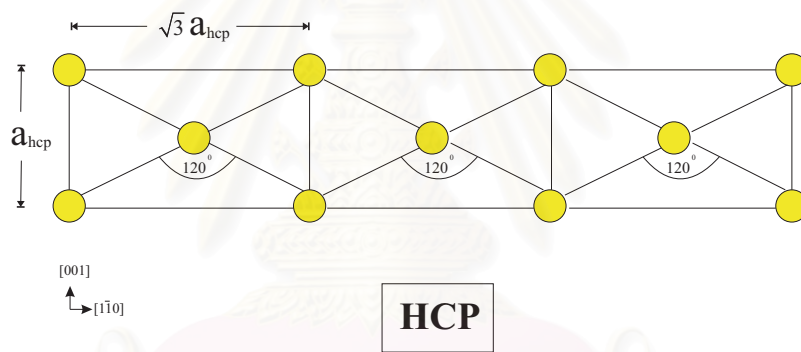


Figure 1.5: The atomic positions in the hexagonal close-packed in  $(0001)_{\text{hcp}}$

A layer of hexagonal close-packed in  $(0001)_{\text{hcp}}$  comes from a layer in  $(110)_{\text{bcc}}$  plane in body centered cubic. The orientation relations are

$$(110)_{\text{bcc}} \parallel (0001)_{\text{hcp}}, \quad (1.1)$$

and

$$[\bar{1}\bar{1}0]_{\text{bcc}} \parallel [1\bar{1}00]_{\text{hcp}}. \quad (1.2)$$

Consequently, we obtain the hcp structure from the bcc-hcp phase transition. It is shown in Fig.(1.6)

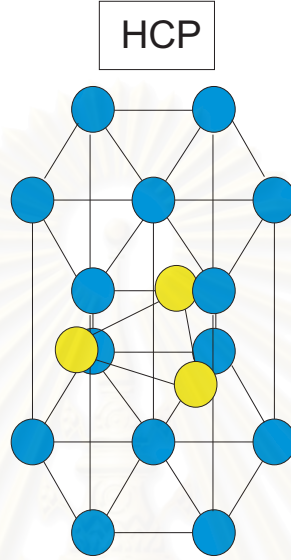


Figure 1.6: The hexagonal close-packed structure

Theoretical models have been proposed in order to explain the experimental results. The neutron scattering experiments, by Pretry, *et.al.*[4] measured the phonon dispersion curves for bcc Ti at 1293K. They found that the frequencies for the bcc phase at  $[\xi\xi0]$   $T_1$  phonon branch are very low and real. In conjunction with these experimental measurements, Ye, *et.al.*[5] studied the phonon-phonon coupling from first-principles total-energy calculations. They found that the harmonic frequency for the  $T_1 N$ -point phonon is imaginary at  $T = 0K$ . It shows the instability for the bcc phase at  $[\xi\xi0]$   $T_1$  phonon branch. Therefore, it has been believed that they are stabilized by the anharmonic effects at high temperature. Moreover,  $[\xi\xi0]$   $T_1$  phonon branch is suggested to be the cause of the  $\alpha$ - $\beta$  phase transition which corresponds with **Burger's distortions**[2].

The  $\alpha$ - $\beta$  phase transition is an important phenomenon. In this work, the phase transition is a **first-order transition** because the total entropy and the total volume of the system expand discontinuously at the transition temperature. From molecular dynamics simulations, we calculated the volume of the bcc and hcp phases at  $T_0 = 1155K$  and they are  $26.177 \text{ \AA}^3/\text{atom}$  and  $17.623 \text{ \AA}^3/\text{atom}$  respectively. The phase transition affects the properties such as the hardening and softening, and it leads to the Shape Memory Effect (SME). In this work, we are interested in calculating the transition temperature. In experiments[4], Petry, *et.al* found that Ti exhibits the transition temperature at 1,155K. We observe that the transition temperature occurs at a high temperature. So, the computer simulation is used to calculate the transition temperature and to study the transition mechanism.

The calculations of the transition temperature of Ti using the computer simulation was studied by Moroni, *et. al.*[6]. They used an *ab initio* method to calculate the Gibbs free energy difference of the electronic part, i.e. only  $\Delta G_E$ . The transition temperature was obtained from the condition that at such a temperature  $\Delta G_E$  must be equal to zero. It was found to be approximately 2,050K. Craievich, *et. al.*[7] calculated the transition temperature which was approximately 3,350K from the electronic free energy difference only. The calculated transition temperature from Moroni, *et. al.*[6] and Craievich, *et. al.*[7] are not in good agreement with the experimental value. We believe that the cause of this disagreement comes from neglecting the contributions of thermal lattice vibrations. From experimental results [4, 8] and theoretical calculations [9], the contribution of thermal lattice vibrations are much larger than thermal electronic contribution. So, thermal lattice vibrations are important part and cannot be neglected. In this research, the Helmholtz free energies of the systems include the thermal lattice vibrations and thermal electronic part to improve the calculation of the transi-

tion temperature. We calculate the Helmholtz free energy by using the molecular dynamics (**MD**) which is a method to study the classical motion of many-body system.

The outline of this thesis is as follows: In Chapter II, we will describe the process of the molecular dynamics method. In addition, the Finnis-Sinclair potential energy, used to represent the potential energy of Ti, will be explained. From both theoretical and experimental methods [4, 9, 10], it is found that the bcc to hcp phase transition of Ti occurs due to the vibrational entropy and the electronic entropy. The calculations of the vibrational entropy and electronic entropy will be presented in Chapter III. In Chapter IV, we will show the results of the potential energy, the harmonic vibration entropy, the anharmonic vibration entropy and the electronic entropy. The last Chapter is the conclusions of this research.



สถาบันวิทยบริการ  
จุฬาลงกรณ์มหาวิทยาลัย

# CHAPTER II

## MOLECULAR DYNAMICS

### METHOD

In this chapter, we discuss **molecular dynamics simulation**. It is a computer simulation method which calculates interactions among atoms. A trajectory of a particle can be calculated by integrating its equation of motion. In addition, molecular dynamics method can be applied to calculate thermodynamic properties such as potential energy, pressure, phonon frequencies, lattice expansion. The fundamental of molecular dynamics is described in Section 2.1. The potential energy and the kinetic energy calculated from the molecular dynamics method are shown in Section 2.2 and 2.3. Finally, we discuss the pressure in Section 2.4.

#### 2.1 General Description of The MD Method

In order to study several properties of condensed matter or the structural phase transformation, one of methods in theoretical study of classical motion of atoms is **molecular dynamics**(MD). MD method is a computational method for studying classical motions of many-body systems. This computational method provides detail information of the trajectory of each particle obtained by solving Newton's second law.



$$\vec{F}_i = m_i \vec{a}_i, \quad i = 1, 2, \dots, N, \quad (2.1)$$

for each atom  $i$  in an  $N$ -body system,  $m_i$  is the atom mass, and  $F_i$  is the total force due to the interactions with other atoms acting upon it. Conventionally, MD simulation conserves the total energy and the linear momentum.

The process of a MD program is described as following; first, we construct MD simulation box with a crystal structure. At  $t = 0$ , We set initial positions, velocities and accelerations of each atom. The positions are placed on lattice sites. The initial velocities are defined from **Maxwell distribution** at a certain temperature  $T$ . The acceleration comes from the forces and the forces come from the interatomic potential defined in Section 2.2. In the second step, we evaluate trajectory at a later time  $t + \delta t$ . The positions, velocities and accelerations at  $t + \delta t$  of all atoms will be predicted **Taylor expansion**. We chose a good integration method which is the heart of the MD method to find a correct quantity. The **Gear predictor-corrector** algorithm is chosen in this work. (we discuss the detail of the Gear predictor-corrector method later.) The next step, we compute the atomic forces by taking derivative of the potential energy at the predicted positions with respect to the change in the atomic positions:

$$\vec{F}_i = -\frac{dE_i}{dr_i} \hat{r}_i. \quad (2.2)$$

where  $E_i$  is the potential energy of atom  $i$  which is constructed from the relative positions of the atoms. In this study, we use **Finnis-Sinclair potential** [2],[11] for Ti (see Section 2.2). Consequently, the accelerations are estimated from the atomic forces

$$\vec{a}_i = -\frac{1}{m_i} \cdot \frac{dE_i}{dr_i} \hat{r}_i. \quad (2.3)$$

Lastly, The difference between the accelerations and the predicted accelerations is calculated and added to the predicted trajectories. Therefore, we obtain the true trajectories, velocities, and acceleration at  $t + \delta t$ . The over all process of MD can be shown in Fig.(2.1).

From the flow chart, it is easy to see that the system 's energy can be monitored instantaneously. When the system reaches an equilibrium, we can calculate the average or equilibrium energy. The instantaneous velocities lead to calculation of temperature and information on phonon states. Hence, MD provides essential quantities for studying the phase transition.

### 2.1.1 Gear Predictor-Corrector method

This section describes an integration method for finding the atomic trajectories which is the heart of the MD method. The type of our problem is **Ordinary Differential Equations (ODE)** that can be solved by numerical methods such as Euler 's method, Runge-Kutta methods, Heun 's method, Gear Predictor-Corrector method, etc. For a problem which has complicated functions, it requires a suitable algorithm. In this work, we have chosen **Gear Predictor-Corrector** method [12] due to its simple forms and its efficiency. The true atomic trajectories at  $t + \delta t$  can be calculated from the past function values (the positions, velocities and accelerations at  $t$ ).

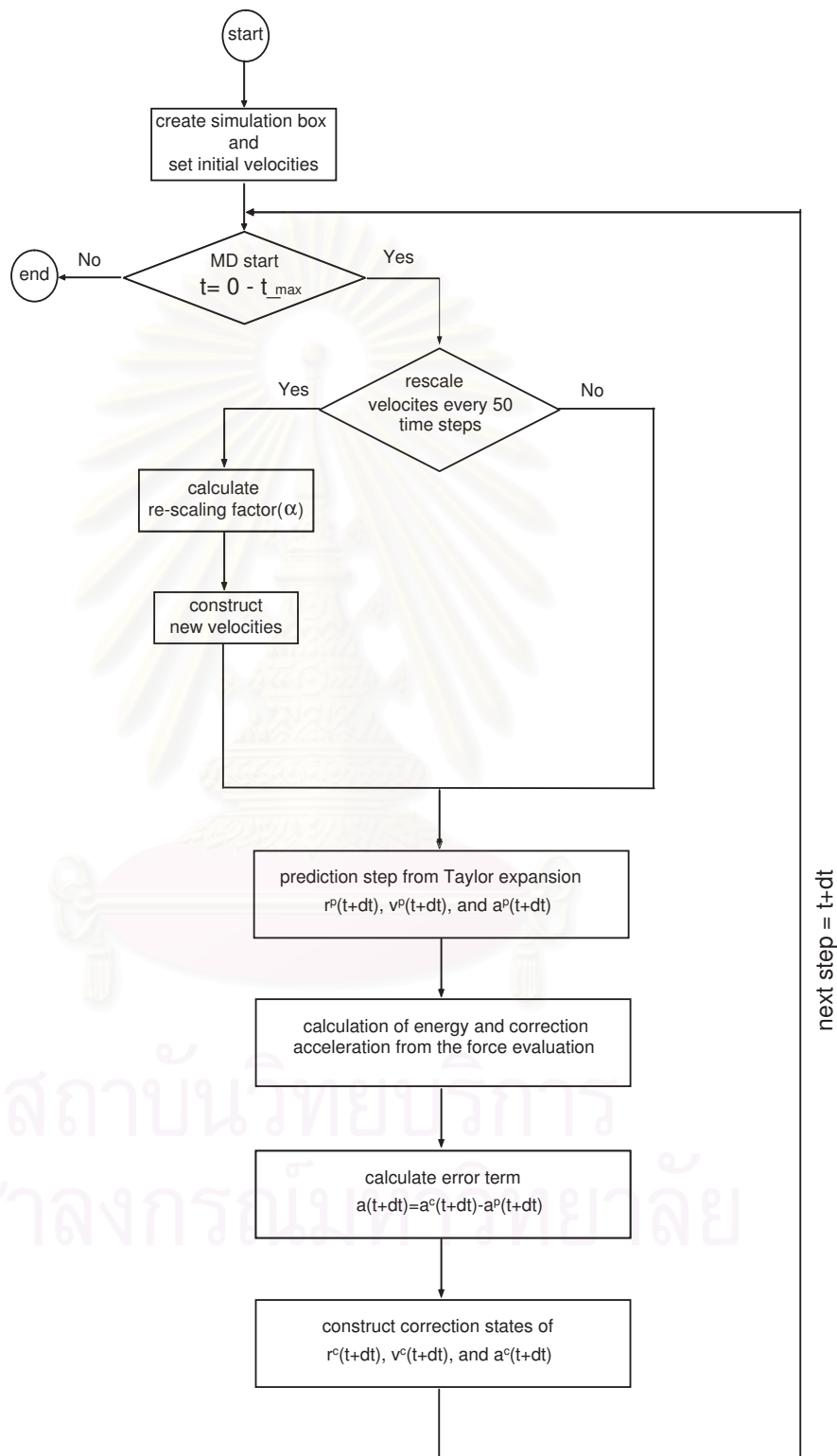


Figure 2.1: Flow chart of the MD simulation

The atomic trajectories are estimated as follows: firstly, at each timestep ( $\delta t$ ), the next atomic trajectories such as the positions, velocities, and accelerations are predicted using **Taylor expansion**. It can be written as

$$r^p(t + \delta t) = r(t) + \delta t \cdot v(t) + \frac{1}{2}\delta t^2 \cdot a(t) + \frac{1}{6}\delta t^3 \cdot b(t) + \dots \quad (2.4)$$

$$v^p(t + \delta t) = v(t) + \delta t \cdot a(t) + \frac{1}{2}\delta t^2 \cdot b(t) + \dots \quad (2.5)$$

$$a^p(t + \delta t) = a(t) + \delta t \cdot b(t) + \dots \quad (2.6)$$

$$b^p(t + \delta t) = b(t) + \dots \quad (2.7)$$

or this can be written in a matrix form of fourth-order Gear predictor-corrector

$$\begin{bmatrix} r^p(t + \delta t) \\ v^p(t + \delta t) \\ a^p(t + \delta t) \\ b^p(t + \delta t) \end{bmatrix} = \begin{bmatrix} 1 & \delta t & \frac{1}{2}\delta t^2 & \frac{1}{6}\delta t^3 \\ 0 & 1 & \delta t & \frac{1}{2}\delta t^2 \\ 0 & 0 & 1 & \delta t \\ 0 & 0 & 0 & 1 \end{bmatrix} \begin{bmatrix} r(t) \\ v(t) \\ a(t) \\ b(t) \end{bmatrix}, \quad (2.8)$$

The superscript  $p$  indicates **predicted values** which are not correct trajectories at  $t + \delta t$ . Note that  $r$ ,  $v$ ,  $a$  and  $b$  are positions, velocities, accelerations and the third time derivatives of position respectively. This is called the **predictor step**. These values in Eq.(2.8) are kept for calculating in the final step. In the next step, we calculate an error in the predictor step which is obtained from the difference between the corrected and predicted accelerations, written as

$$\Delta a(t + \delta t) = a^c(t + \delta t) - a^p(t + \delta t). \quad (2.9)$$

The superscript  $c$  indicates **corrected values**,  $a^c$  is the corrected acceleration which can be solved by using the true force at the time  $t + \delta t$  and the information from the prediction step. The true force is evaluated by taking the gradient of the potential in Eq.(2.2) and the potential is calculated by using Equation (2.12) and the predicted positions. In final step, the true trajectories can be considered from the sum of the values of the predictor step which are provided in the beginning step and the error in the predictor step. This is **called the corrector step**. This can be written in a vector form

$$\begin{bmatrix} r^c(t + \delta t) \\ v^c(t + \delta t) \\ a^c(t + \delta t) \\ b^c(t + \delta t) \end{bmatrix} = \begin{bmatrix} r^p(t + \delta t) \\ v^p(t + \delta t) \\ a^p(t + \delta t) \\ b^p(t + \delta t) \end{bmatrix} + \begin{bmatrix} C_0 \\ C_1 \\ C_2 \\ C_3 \end{bmatrix} \Delta a(t + \delta t), \quad (2.10)$$

In this equation,  $C_0, C_1, C_2$  and  $C_3$  are a constant vector. The choice of  $C_0, C_1, C_2$  and  $C_3$  are depended on the orders of the method and resulted in stability properties [12]. Gear [13] derived the best coefficients  $C_0, C_1, C_2$  and  $C_3$  equal to  $\frac{1}{6}, \frac{5}{6}, 1$  and  $\frac{1}{3}$  respectively, considering the optimum stability and the precision of the solution.

### 2.1.2 Choice of a time step

The choice of each time-step ( $\delta t$ ) is important because if we choose too large  $\delta t$  then the system would be unstable, i.e. the total energy is not conserved, but for too small  $\delta t$ , the systems would take unnecessary long time for integration. For the simulations of solid states physics,  $\delta t$  should be much shorter than the period

of typical phonons. Ackland [14] discussed the stability of the Gear predictor-corrector scheme with various  $\delta t$ . He found that  $\delta t$  should be smaller than 5 fs. In this work, we use  $\delta t = 1$ fs.

## 2.2 The Potential Energy for Titanium

The cohesive energy of a crystal is defined as the potential energy of a solid required to break atoms of the solid into isolated atomic species. The cohesive energy of the crystalline elements is depended on types of interactions, for example, Van der Waals-London interaction for the inert gases, covalent bond for covalent crystals and ionic bond for ionic crystals. For transition metals, we choose Finnis-Sinclair potential to represent the potential energy because it gives a good descriptions for the hcp and bcc phases in transition metals [11].

In **Finnis-Sinclair scheme** [11], the cohesive energy consists of two components, i.e the repulsive part ( $E_{rep}$ ) is repulsive energy due to the screened coulomb interaction which is short-range interaction because of the screening effect in metals. The attractive part ( $E_{bond}$ ) is attractive bonding energy due to the interaction among nuclei and the free electrons. The cohesive energy is written as

$$E_{coh} = E_{rep} + E_{bond}. \quad (2.11)$$

For a transition metal, **Finnis-Sinclair** (1984) suggested a functional form of potentials [11] as in Eq.(2.12) and then fitted it to empirical data such as cohesive energies and elastic constants to make a potential of metals. In this work, we use Finnis-Sinclair potential which has assumed a cubic spline form [2],[15],[16]. This can be written as



$$E_i = \frac{1}{2} \sum_j V(r_{ij}) - \rho_i^{\frac{1}{2}}, \quad (2.12)$$

where,

$$\rho_i = \sum_j \phi(r_{ij}), \quad (2.13)$$

where  $E_i$  is the potential energy of the  $i^{\text{th}}$  atom.  $V(r_{ij})$  and  $\phi(r_{ij})$  are pairwise function between atom  $i$  and one of the other atoms  $j$ . In Eq.(2.12), the first term is a short-range potential repulsive energy represented by a sum of a repulsive pair potential. The other term is the attractive bonding energy. Each term is defined as

$$V(r) = \sum_{k=1}^6 A_k (R_k - r_{ij})^3 H(R_k - r_{ij}), \quad (2.14)$$

and

$$\rho_i = \sum_j \sum_{k=1}^2 a_k (r_k - r_{ij})^3 H(R_k - r_{ij}). \quad (2.15)$$

where  $r_{ij}$  is the distance between atoms  $i$  and  $j$  and  $A_k$ ,  $R_k$ ,  $a_k$  and  $r_k$  are fitting parameters, which are shown in table (2.1).  $H(R_k - r)$  is **the heaviside step function** defined as

$$H(R_k - r_{ij}) = \begin{cases} 0 & \text{if } r_{ij} > R_k; \\ 1 & \text{if } r_{ij} \leq R_k. \end{cases} \quad (2.16)$$

Eq.(2.12) can be used to calculate the potential energy of titanium. In this study, the number of atoms in the bcc phase is 8,192 atoms and the number of atoms in the hcp phase is 6,912 atoms. The temperature is constrained to a constant. The time evolution is continued until  $t_{max} = 30ps$ . Typical simulation results of the

$k$	$A_k(eV/\text{\AA}^3)$	$R_k(\text{\AA})$	$a_k(eV^2/\text{\AA}^3)$	$r_k(\text{\AA})$
1	-0.59795742	5.09113442	0.41675387	5.57630036
2	0.84548534	5.00763200	-0.41953298	4.79927490
3	-0.22789207	4.67382832	-	-
4	-0.10887478	3.6440795	-	-
5	0.78041828	3.3384488	-	-
6	0.37613482	2.95080065	-	-

Table 2.1: Fitting parameters  $k$ ,  $A_k$ ,  $R_k$ ,  $a_k$  and  $r$  for titanium [11]

potential energy in the hcp phase at 1,200K are presented in Fig.(2.2) and Fig. (2.3) for the bcc phase at 900K .

Hence, we observe the potential energy of the bcc phase and the hcp phase from the MD simulation. Both phases show non-equilibrium states at the beginning. After the system is evolved for a few picosecond, it approaches the thermodynamic equilibrium. In addition, from Fig.(2.3), we find that the energy of the bcc phase is constant for a short period, then the tendency of the potential energy is decreasing and reaching a new equilibrium. This is because the simulations have been set to the bcc structure at beginning. However,  $T=900\text{K}$  is lower than the transition temperature  $T_0 = 1,155\text{K}$  [4],[10]. Hence, the system undergoes a phase transition from bcc to hcp phase. From MD, we find that the phase transition does not happen at  $T = 1,000\text{ K}$ ,  $1,100\text{K}$ ,  $1,200\text{K}$ , and  $1,300\text{ K}$ . It is worth mentioning that we observe no hcp to bcc transition.

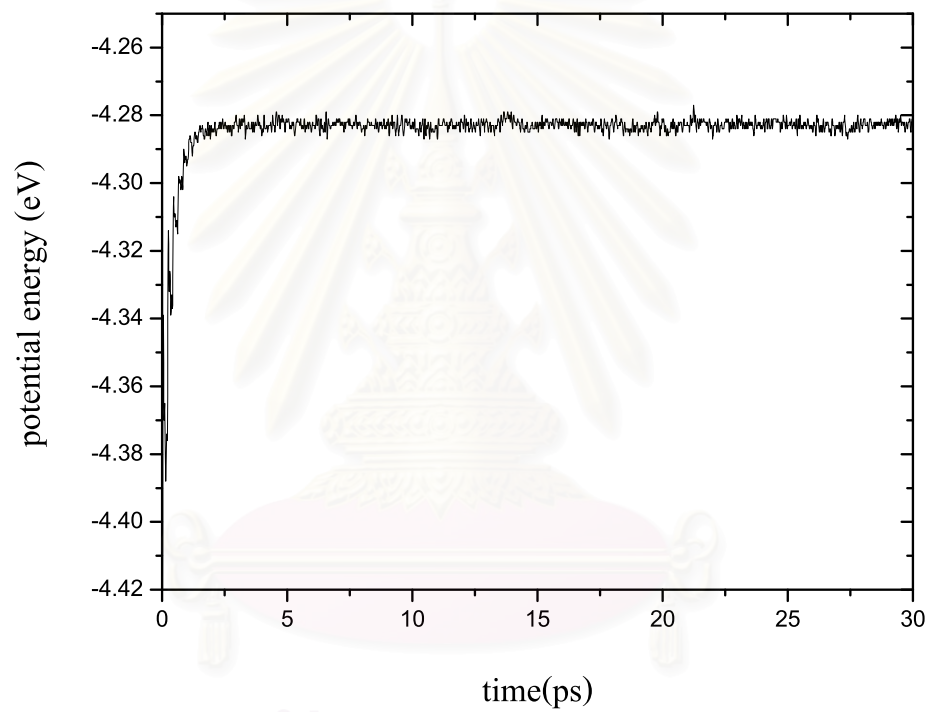


Figure 2.2: The potential energy of the hcp phase at 1,200K

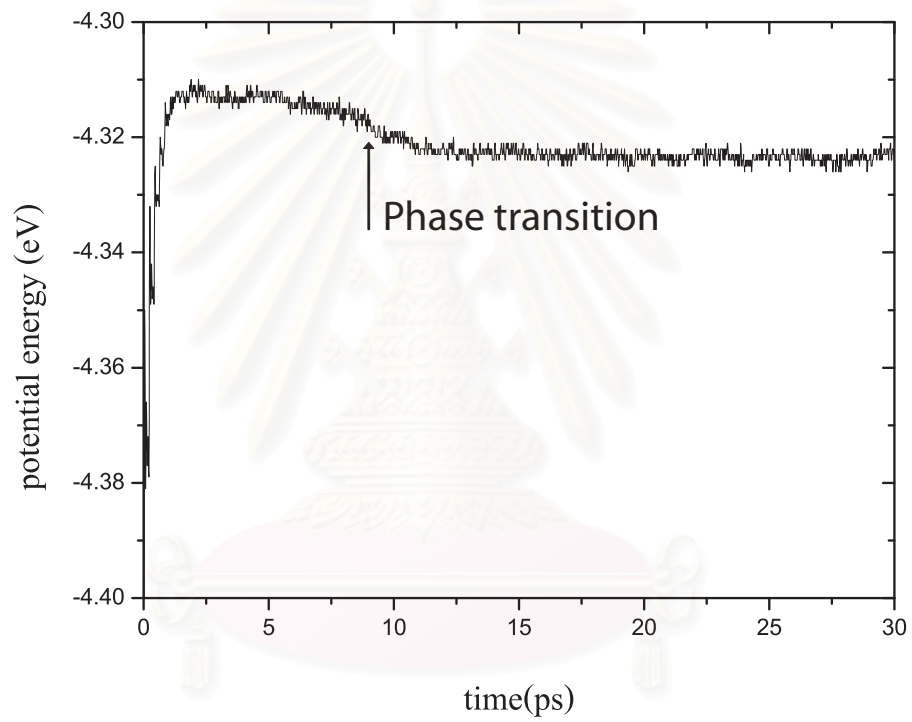


Figure 2.3: The potential energy of the bcc phase at 900K

สงขลานครินทร์  
จุฬาลงกรณ์มหาวิทยาลัย

Moreover, the interatomic potential energy is an important part which it is used to describe the harmonic vibrational part and the anharmonic vibrational part. Figure 2.4 shows a typical interatomic potential energy. It can be seen that there is a value of displacement ( $r$ ) which corresponds to the interatomic potential energy. It exists a local minimum at  $r_0$  which is the equilibrium position of the neighboring atom. We found that atoms move only a little from their equilibrium sites at low temperature. From the figure, we can estimate the potential around the local minimum by a quadratic function. Consequently, the interaction is spring-like and the small vibration is purely harmonic. At high temperature, atoms move further away from their equilibrium sites. The potential deviates from a quadratic function and has no symmetry. The vibration is no longer small and becomes the so-called anharmonic vibration.

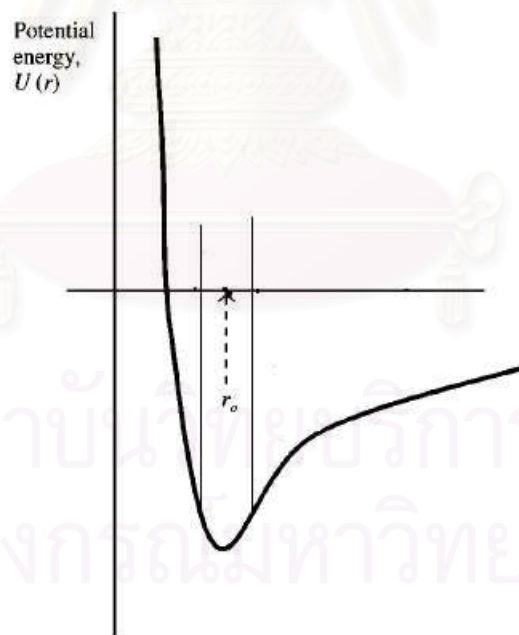


Figure 2.4: Typical of the potential energy curve

## 2.3 The Kinetic Energy

In MD simulations, the kinetic energy of system [18] is obtained from the velocities of all atoms at each time  $t$ . This can be written as

$$K(t) = \frac{1}{2} \sum_i^N m_i v_i^2(t), \quad (2.17)$$

where  $K(t)$  is the kinetic energy,  $m_i$  is the atom mass, and  $v_i$  is the velocity of atom  $i$ . The kinetic energy is an important part because it can be directly related to temperature  $T$ . From equipartition theorem [19],[21], the average kinetic energy is equal to  $k_B T/2$  per degree of freedom. For a monoatomic element, the total kinetic energy is

$$K(t) = \frac{3}{2} N k_B T_{instan}(t), \quad (2.18)$$

where  $T_{instan}(t)$  is the instantaneous temperature at time  $t$ ,  $N$  is the number of atoms in the simulation box, and  $k_B$  is Boltzmann's constant. Then, at each timestep, the temperature can be measured from MD simulation. From Eq.(2.17) and (eq.2.18), the temperature of the system is defined as

$$\frac{3}{2} N k_B T_{instan}(t) = \frac{1}{2} \sum_i^N m_i v_i^2(t), \quad (2.19)$$

thus,

$$T_{instan}(t) = \frac{1}{3Nk_B} \sum_i^N m_i v_i^2(t). \quad (2.20)$$

In this work, we try to calculate several thermodynamic variables using MD simulation under various constant temperatures. Thus we need a tool to keep a

constant temperature. From the relationship between the kinetic energy  $K(t)$  and the instantaneous temperature  $T_{instan}(t)$ , Eq.(2.20) can bring the system from any constant temperature to a required temperature. At the starting of simulations, the velocity of particles can be generated from Maxwell-Blotzmann distribution. In addition, the initial particle velocities must obey the conservation of linear momentum, i.e.  $\sum_i m_i v_i = 0$ . We obtain the temperature at the starting time as

$$\frac{3}{2}Nk_B T_0 = \frac{1}{2} \sum_i m_i v_i^2(0), \quad (2.21)$$

where  $T_0$  is the started temperature and  $v_i(0)$  is represented by the set of initial velocities for each atom  $i$  at the starting time. The system moves toward an equilibrium at the attentive temperature  $T$  by multiplying a factor ( $\alpha$ ).

$$\alpha^2 \sum_i \frac{1}{2} m_i v_i^2(0) = \frac{3}{2} N k_B T, \quad (2.22)$$

where  $\alpha$  is called re-scaling factor and  $T$  is the required temperature. The re-scaling factor  $\alpha$  can be written as

$$\alpha = \sqrt{\frac{T}{T_0}}. \quad (2.23)$$

Therefore, if we are interested in the states of a system at a required temperature, we can change the temperature of the simulation by multiplying the re-scaling factor to Eq.(2.21). The re-scaling factor cannot be multiplied every time-step. Otherwise the system will be constrained too much and the dynamics of system will be incorrect.



## 2.4 Measuring The Pressure

In order to evaluate the pressure in the MD simulation, we use the Clausius virial function [1],[18]. This important result is known as the virial Equation written as

$$PV = Nk_B T + \frac{1}{3} \left\langle \sum_{i=1}^N \vec{r}_i \cdot \vec{F}_i \right\rangle, \quad (2.24)$$

where  $P$  is the pressure of the system,  $V$  is the volume of the simulation box,  $T$  is the constant temperature,  $\vec{r}_i$  is displacement of atom  $i$  and  $\vec{F}_i$  is the internal force which is arising from the interatomic interaction. We can reduce Eq.(2.24) to the well-known equation of states of the perfect gas if the particles are non-interacting i.e.  $\vec{F} = 0$ . In this work, the interactions between the particle and others are evaluated via the potential Eq.(2.2) and Eq.(2.12). We can calculate the pressure using Eq.(2.24), which is easily accessible in the MD simulation.

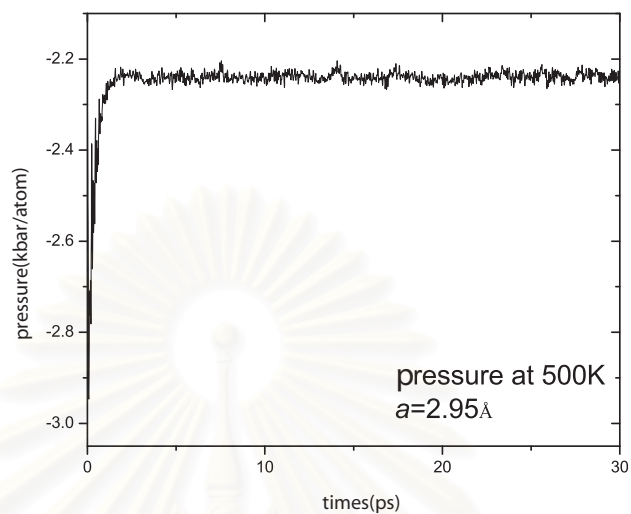
At each timestep, we calculate the pressure from the MD simulation at the various temperatures using Eq.(2.24). From Figure 2.5 (a), it shows the pressure as a function of time for the hcp phase at constant temperature  $T = 500\text{K}$  and lattice constant  $a = 2.95 \text{ \AA}$ . The average pressure is  $-2.239 \text{ kbar/atom}$  at an equilibrium state. We also illustrate the relation between the pressure and the lattice parameter at constant temperature in Figure 2.5 (b). We find that the changing of the pressure of the system is locally linear with the lattice constant.

Furthermore, we can evaluate **the true lattice constant** at each temperature from the relation between the pressure and the lattice constant. At each temperature, the true lattice will be determined from the lattice constant having the zero pressure ( $P = 0$ ). Because the zero pressure means that the simulation box does not have the total work, which comes from the thermal energy, acting on the simulation box 's walls. For instance, the true lattice constant of the hcp

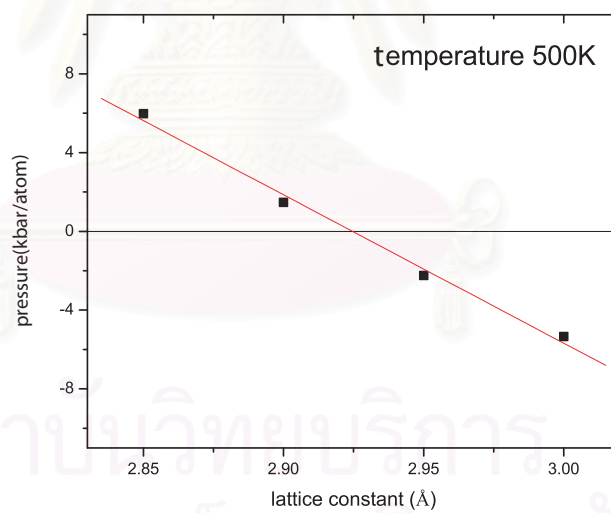
phase at  $T = 500\text{K}$  is calculated via the linear fit of the data points. The average pressure is calculated at the constant temperature  $T = 500\text{K}$  and lattice constant  $a = 2.85 \text{ \AA}$ ,  $2.9 \text{ \AA}$ ,  $2.95 \text{ \AA}$ , and  $3.0\text{\AA}$ . The results are shown in Figure 2.5 (b). The true lattice constant at  $P = 0$  is  $2.92 \text{ \AA}$ . We calculate the true lattice constant at constant temperature between  $300\text{K} - 1300\text{K}$  of the bcc and hcp phases. These values of the true lattice constant will be used for calculating other thermodynamic properties, i.e. Helmholtz free energy from the MD simulations. The results will be presented in Chapter IV.



สถาบันวิทยบริการ  
จุฬาลงกรณ์มหาวิทยาลัย



(a)



(b)

Figure 2.5: a) the pressure of the hcp phase from the MD simulation at 500K and lattice constant =  $2.95\text{\AA}$ . b) the pressure-lattice constant relationship of the hcp phase at 500K

# CHAPTER III

## THE TOTAL ENTROPY

In this chapter, we discuss the total entropy which has an important role for the occurrence of the  $\alpha$ - $\beta$  phase transition. The entropy of a crystal [9] is composed of vibrational entropy ( $S_{vib}$ ) which includes the harmonic vibrational entropy ( $S_H$ ), the anharmonic vibrational entropy ( $S_A$ ), and the electronic entropy ( $S_E$ ). It can be written as

$$S = S_H + S_A + S_E. \quad (3.1)$$

We explain how to apply statistical methods to find the total entropy. We discuss the harmonic vibrational entropy in Section 3.1 and the anharmonic vibrational entropy in Section 3.2. Finally, the electronic entropy is shown in Section 3.3.

### 3.1 Harmonic Vibrational Entropy

In this section, we discuss the method which is used to calculate the harmonic vibrational entropy from the **MD** method. We apply statistical methods to calculate the harmonic vibrational entropy via **partition function**[19] of a system. The **partition function** is a sum over all states appearing in the system. It is

written as

$$\mathcal{Z}(T, V, N) = \sum_{N=0}^{\infty} \left[ \exp(-\beta \sum_{r=1}^{\infty} E_{Nr}) \right], \quad (3.2)$$

and

$$\beta = \frac{1}{k_B T}. \quad (3.3)$$

where  $\mathcal{Z}(T, V, N)$  is the partition function at constant temperature, constant volume, and constant number of particles,  $k_B$  is the Boltzmann constant,  $N$  is the number of particles in the system, and  $E_{Nr}$  is the energy of state  $r$ .

In **Debye's theory**, a crystal consisting of  $N$  atoms has  $3N$  degrees of freedom corresponding to  $3N$  coordinates required to specify the positions of the atoms. The atoms in this crystal can be assumed as oscillators. If the system received the energy from an external source, the atoms will vibrate. This can be described in terms of  $3N$  normal modes of vibration of the crystal. The energy of the crystal can be solved by using quantum mechanics. We have dropped the zero point energy of the oscillators because it does not affect the calculation of the free energy. The energy of a harmonic oscillator of frequency  $\omega$  is

$$\epsilon = n\hbar\omega, \quad n = 0, 1, 2, 3, \dots \quad (3.4)$$

where  $\hbar$  is the Planck constant divided by  $2\pi$ . The integer  $n$  is the discrete energy level of a harmonic oscillator. The states of the particles in the system are specified by a set of occupation numbers  $n_1, n_2, \dots, n_r, \dots$  of each of states with the energies  $\epsilon_1 \leq \epsilon_2 \leq \dots \epsilon_r \leq \dots$  or  $\hbar\omega_1 \leq \hbar\omega_2 \leq \dots \hbar\omega_r \leq \dots$ . The summation over all the occupation numbers is given by

$$\sum_r n_r = 3N. \quad (3.5)$$

The total energy can be written as

$$E_{Nr} = \sum_r n_r \epsilon_r \quad \text{or} \quad n_1 \hbar \omega_1 + n_2 \hbar \omega_2 + \dots + n_r \hbar \omega_r + \dots \quad (3.6)$$

So, the totality of such sets of occupation numbers defines all possible states of the system. We can change Eq.(3.2) into

$$\mathcal{Z}(T, V, N) = \sum_{n_1, n_2, \dots} \left[ \exp(-\beta \sum_{r=1}^{\infty} n_r \epsilon_r) \right], \quad (3.7)$$

Substituting Eq.(3.6) into Eq.(3.7), we obtain the the partition function of the system which is used to estimate the free energy of system.

$$\begin{aligned} \mathcal{Z}(T, V, N) &= \sum_{n_1, n_2, \dots} \exp \{ (-\beta n_1 \hbar \omega_1) + (-\beta n_2 \hbar \omega_2) + \dots \} \\ &= \left\{ \sum_{n_1} \exp(-\beta n_1 \hbar \omega_1) \right\} \cdot \left\{ \sum_{n_2} \exp(-\beta n_2 \hbar \omega_2) \right\} \cdot \dots \end{aligned} \quad (3.8)$$

where  $n_1, n_2, \dots$  cover the range  $0, 1, 2, \dots$  because the particles in the system are bosons. We can write the partition function as

$$\mathcal{Z}(T, V, N) = \prod_{i=1}^{\infty} \mathcal{Z}_i(T, V, N), \quad (3.9)$$

with

$$\mathcal{Z}_i(T, V, N) = \sum_{n_i} \exp(-\beta n_i \hbar \omega_i). \quad (3.10)$$

So, The free energy of the system ( $F_H$ ) is calculated from the partition function. We use the relation in thermodynamics, i.e.

$$F = -\frac{1}{\beta} \ln \mathcal{Z}, \quad (3.11)$$

Substituting Eq.(3.9) into Eq.(3.11),

$$F_H = k_B T \sum_{\omega_i} \ln(1 - \exp^{-\beta \hbar \omega_i}). \quad (3.12)$$

For a system kept at constant temperature or constant volume, the entropy ( $S$ ) is calculated by Maxwell relations[21],

$$S = - \left( \frac{\partial F}{\partial T} \right)_v. \quad (3.13)$$

Therefore, the harmonic free energy is obtained from the sum over all harmonic oscillators which equal to  $3N$  harmonic oscillator. The harmonic vibrational entropy ( $S_H$ ) can be calculated by Equation (3.13).  $S_H$  is written as

$$S_H = -k_B \sum_{i=1}^{3N} \{f(\omega_i) \ln f(\omega_i) - [1 + f(\omega_i)] \ln[1 + f(\omega_i)]\}, \quad (3.14)$$

where,

$$f(\omega_i) = \left[ \exp\left(\frac{\hbar \omega_i}{k_B T}\right) - 1 \right]^{-1}, \quad (3.15)$$



and  $f(\omega_i)$  is **Bose-Einstein distribution**. We can change from the discrete form to a continuous form. We use  $\omega$  to replace  $\omega_i$ . If we consider the frequencies which have a very small change  $d\omega$ . Consequently, the system possesses  $3N$  oscillators or  $3N$  modes in crystal.

$$S_H = -3Nk_B \int_0^{\omega_{max}} d\omega D(\omega) \{f(\omega) \ln f(\omega) - [1 + f(\omega)] \ln[1 + f(\omega)]\}. \quad (3.16)$$

The total harmonic vibrational entropy can be approximated by an integral over the total frequency between 0 to  $\omega_{max}$ .  $D(\omega)$  is the phonon density of states. If  $D(\omega)$  of the bcc phase and hcp phase are known at constant temperature, the  $S_H$  will directly be estimated from Equation (3.16). Next, we discuss the method to calculate the phonon density of states  $D(\omega)$  of each structure at constant temperature from MD.

สถาบันวิทยบริการ  
จุฬาลงกรณ์มหาวิทยาลัย

### 3.1.1 Phonon density of states in the bcc and hcp phases

The phonon density of states  $D(\omega)$  is used to estimate the harmonic vibrational entropy in Eq.(3.16).  $D(\omega)$  can be directly calculated from the **MD** simulation. Dickey and Paskin [22] showed that the phonon density of states can be calculated from the atomic velocity autocorrelation function  $\gamma(t)$ . It can be written as,

$$\gamma(t) = \int D(\omega) \cos \omega t d\omega, \quad (3.17)$$

and the fourier transform of  $\gamma(t)$  gives directly the phonon density of states  $D(\omega)$ .

$$D(\omega) = \frac{1}{2\pi} \int \gamma(t) \cos(\omega t) dt. \quad (3.18)$$

Dickey and Paskin assumed that  $\gamma(t)$  can be extracted by a suitable analysis of the correlations in the motion. It is defined as

$$\gamma(t) = \sum_i \frac{\langle v_i(t+t_0) \cdot v_i(t_0) \rangle}{\langle v_i(t_0) \cdot v_i(t_0) \rangle}, \quad (3.19)$$

where  $\sum_i$  is the summation over all the atoms in a simulation box, and  $\langle \dots \rangle$  is a ensemble average.  $v_i(t_0)$  and  $v_i(t+t_0)$  are the velocity of atom  $i$  at time-step  $t_0$  and  $t+t_0$  respectively. These  $v_i$  can be obtained from the **MD** simulation.  $\gamma(t)$  is averaged over different time origins in order to gain statistical reliability. The ensemble average can be written as

$$\langle v_i(t+t_0) \cdot v_i(t_0) \rangle \cong \frac{1}{t_{max}} \sum_{t_0=0}^{t_{max}} v_i(t+t_0) \cdot v_i(t_0), \quad (3.20)$$

and

$$\langle v_i(t_0) \cdot v_i(t_0) \rangle \cong \frac{1}{t_{max}} \sum_{t_0=0}^{t_{max}} v_i(t_0) \cdot v_i(t_0), \quad (3.21)$$

Substituting Eq.(3.20) and Eq.(3.21) into Eq.(3.22),

$$\gamma(t) = \sum_i \left( \frac{\sum_{t_0=0}^{t_{max}} v_i(t+t_0) \cdot v_i(t_0)}{\sum_{t_0=0}^{t_{max}} v_i(t_0) \cdot v_i(t_0)} \right). \quad (3.22)$$

In our MD simulations, the velocity autocorrelation can be estimated from Equation 3.22 and is shown in Figure 3.1 (a) for hcp phase at 1,000K. The phonon density of states for hcp phase at  $T = 1,000\text{K}$  can be calculated from Fourier transform, Eq.(3.18), of  $\gamma(t)$  function which is shown in Fig.3.1 (b). For a given  $D(\omega)$ , the harmonic vibrational entropy can be calculated using Eq.(3.16) at various temperatures such as at  $T = 1,000\text{K}$ . We found that  $S_H$  is  $7.69 k_B/atom$  for the hcp phase. It is a little higher than the measurement by Petry, et. al [4], which is  $7.66 k_B/atom$ . In addition, the harmonic vibrational entropy is an important part of Helmholtz free energy.

สถาบันวิทยบริการ  
จุฬาลงกรณ์มหาวิทยาลัย

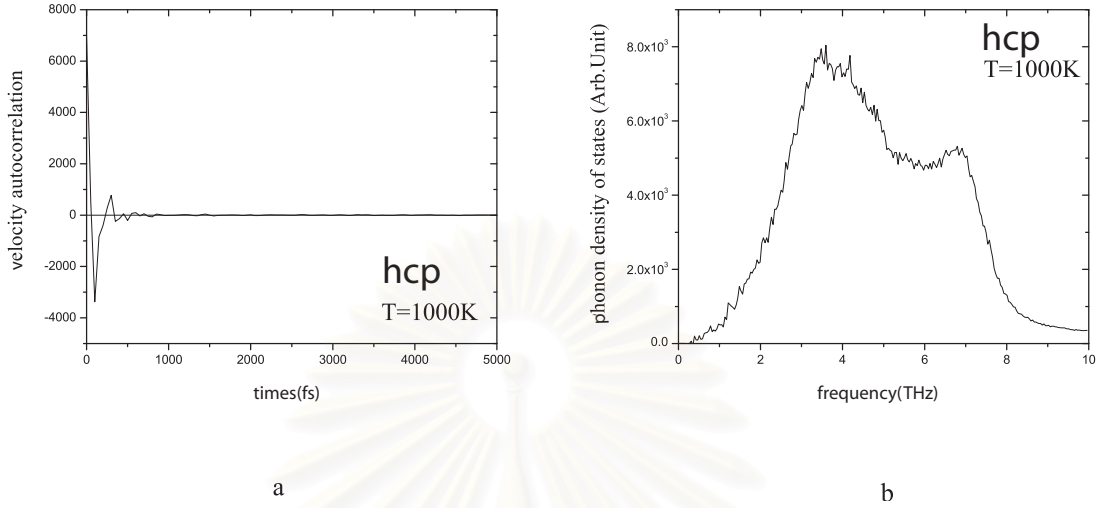


Figure 3.1: a) The velocity autocorrelation  $\gamma(t)$  taken from the hcp phase with 6,912 atoms at 1,000 K, b) the phonon density of states in the hcp phase from the fourier transform of  $\gamma(t)$

## 3.2 Anharmonic Vibrational Entropy

In this section, we discuss the anharmonic effects due to lattice vibrations at high temperature[10]. The anharmonic part arises from phonon-phonon coupling or the coupling among the normal modes. At low temperature, the anharmonic effect can be negligible, but when we increase the temperature, it becomes more important. Ye, *et.al.* [5] studied the phonon-phonon coupling from first-principles total-energy calculations. They found that the harmonic frequency for the  $T_1N$ -point phonon is imaginary. It shows the instability under the harmonic approximation. In conjunction with the experimental measurements, Heiming, *et.al.*[8] found that the frequencies for bcc phase at [110]  $T_1$  phonon branch are very low and real. Thus only harmonic contribution is inadequate. So, we will include the anharmonic part for improving the vibrational entropy.

The anharmonic vibrational entropy ( $S_A$ ) can be solved from the anharmonic free energy. The anharmonic free energy [25] ( $F_A$ ) is defined as

$$\frac{F_A(T, V)}{N-1} = -k_B T \int_{T_0}^T \frac{dT'}{T'} \left[ \frac{[\langle U(T', V) \rangle - U_{min}(V)]}{(N-1)k_B T'} - \frac{3}{2} \right]. \quad (3.23)$$

where  $k_B$  is the Boltzmann's constant,  $U_{min}(V)$  is the potential energy at the atomic positions which minimize the potential energy,  $\langle U(T', V) \rangle$  is the average potential energy at temperature  $T'$ ,  $T_0$  is a low temperature in which the system does not include the anharmonic effects and  $N$  is the number of atoms in the system. The anharmonic vibrational entropy can be obtained exactly from the thermodynamic relation in Eq.(3.13).  $S_A$  is shown to be

$$\frac{S_A}{N-1} = k_B \left[ W(T, V) - \frac{T}{T_0} W(T_0, V) - \frac{3}{2} \left(1 - \frac{T}{T_0}\right) + \int_{T_0}^T \left( W(T', V) - \frac{3}{2} \right) \frac{dT'}{T'} \right], \quad (3.24)$$

where,

$$W(T, V) = \frac{\langle U(T, V) \rangle - U_{min}(V)}{(N-1)k_B T}. \quad (3.25)$$

The anharmonic entropy is calculated at temperatures ranging from  $T=1,000$  K to  $T=1,500$  K between the two phases from Equation (3.24). The values of  $W(T, V)$  are determined from the **MD** simulations.

### 3.3 Electronic Entropy

In this section, we will introduce the electronic entropy ( $S_E$ ) which relates to the electronic band structure. The electronic entropy can be evaluated by **the grand partition function** [23]. The grand partition function is the partition function of the grand canonical ensemble which the system is allowed to exchange particles and energies with environment. A state of the system is specified by three parameters, temperature ( $T$ ), the volume ( $V$ ), and chemical potential ( $\mu$ ). **The grand partition function**  $\mathcal{Z}(T, V, \mu)$  is defined as

$$\mathcal{Z}(T, V, \mu) = \sum_{N=0}^{\infty} \left\{ \sum_{r=1}^{\infty} \exp[\beta(\mu N - E_{Nr})] \right\}. \quad (3.26)$$

where  $\beta$  is  $\frac{1}{k_B T}$ . The system consists of  $N$  particles and possesses energy  $E_{Nr}$ . The states of the particles in the system are specified by a set of occupation numbers  $n_1, n_2, \dots, n_r, \dots$  of each of states with energies  $\varepsilon_1 \leq \varepsilon_2 \leq \dots \varepsilon_r \leq \dots$ . The total particle number and the total energy can be written as

$$N = \sum_r n_r \quad , \quad E_{Nr} = \sum_r n_r \varepsilon_r. \quad (3.27)$$

We can change the summation in Eq.(3.26) into the sum of each occupation number  $n_r$  independently. Substituting Eq.(3.27) into Eq.(3.26), we obtain **the grand partition function**. It can be written as

$$\mathcal{Z}(T, V, \mu) = \sum_{n_1, n_2, \dots} \left\{ \sum_{r=1}^{\infty} \exp[\beta(\mu n_r - n_r \varepsilon_r)] \right\}. \quad (3.28)$$

$$\begin{aligned}
\mathcal{Z}(T, V, \mu) &= \sum_{n_1, n_2, \dots} \exp \{ \beta [ \mu (n_1 + n_2 + \dots) - (n_1 \varepsilon_1 + n_2 \varepsilon_2 + \dots) ] \}, \\
&= \sum_{n_1, n_2, \dots} \exp \{ \beta (\mu - \varepsilon_1) n_1 + \beta (\mu - \varepsilon_2) n_2 + \dots \}, \quad (3.29) \\
&= \left\{ \sum_{n_1} \exp \beta (\mu - \varepsilon_1) n_1 \right\} \cdot \left\{ \sum_{n_2} \exp \beta (\mu - \varepsilon_2) n_2 \right\} \cdot \dots,
\end{aligned}$$

$n_1, n_2, \dots$  cover the range 0, 1 because the particles in the system are fermions which are restricted by **the exclusion principle**; two fermions cannot be in the same state.  $\prod$  is used to denote a product of factors ; e.g.,  $\prod_{r=1}^p a_r = a_1 a_2 \dots a_p$ . We can write **the grand partition function** of the last expression in Equation 3.29 as

$$\mathcal{Z}(T, V, \mu) = \prod_{i=1}^{\infty} \mathcal{Z}_i(T, V, \mu), \quad (3.30)$$

with

$$\mathcal{Z}_i(T, V, \mu) = 1 + \exp \beta (\mu - \varepsilon_i). \quad (3.31)$$

Next, we calculate the free energy of system ( $F_E$ ). From Eq.(3.11) and Eq.(3.30),  $F_E$  is given by

$$F_E = - \sum_i \frac{\ln[1 + \exp \beta (\mu - \varepsilon_i)]}{\beta}. \quad (3.32)$$

The electronic entropy ( $S_E$ ) is calculated by substituting Eq.(3.32) in Eq.(3.13).



We obtain

$$S_E = -k_B \sum_i [1 - f(\varepsilon_i)] \ln [1 - f(\varepsilon_i)] + f(\varepsilon_i) \ln f(\varepsilon_i), \quad (3.33)$$

where,

$$f(\varepsilon_i) = [\exp(\frac{\varepsilon_i - \mu}{k_B T}) + 1]^{-1}. \quad (3.34)$$

Eq.(3.34) is the **Fermi-Dirac distribution**. If the energy levels  $\varepsilon_i$  lie very closely together. Consequently, we can change from a discrete form to a continuous form. Eq.(3.33) reduces to an integral of the electronic density of states  $g(\varepsilon)$  with continuous variable  $\varepsilon$ . The electron-phonon interaction effects are not included in this system.  $S_E$  can be written as

$$S_E = -k_B \int g(\varepsilon) \{ [1 - f(\varepsilon)] \ln [1 - f(\varepsilon)] + f(\varepsilon) \ln f(\varepsilon) \} d\varepsilon. \quad (3.35)$$

If we know the electronic density of states  $g(\varepsilon)$ , the electronic entropy can be evaluated from Eq.(3.35). The electronic structure and the electronic density of states can be calculated from the full-potential linear muffin-tin orbitals (FP-LMTO) method by Ahuja[3], Moroni[6], Erikson[9], Nishitani[27], Paxton[31], the muffin-tin approximation (MT) method by Hygh and Ponal[29], the augmented-plane-wave (APW) method by Welch[30]. In this work, the electronic density of states of Ti is taken from Ahuja, *et. al.*[3]. We display DOS for hcp and bcc in Fig.3.2 and Fig.3.3 respectively.

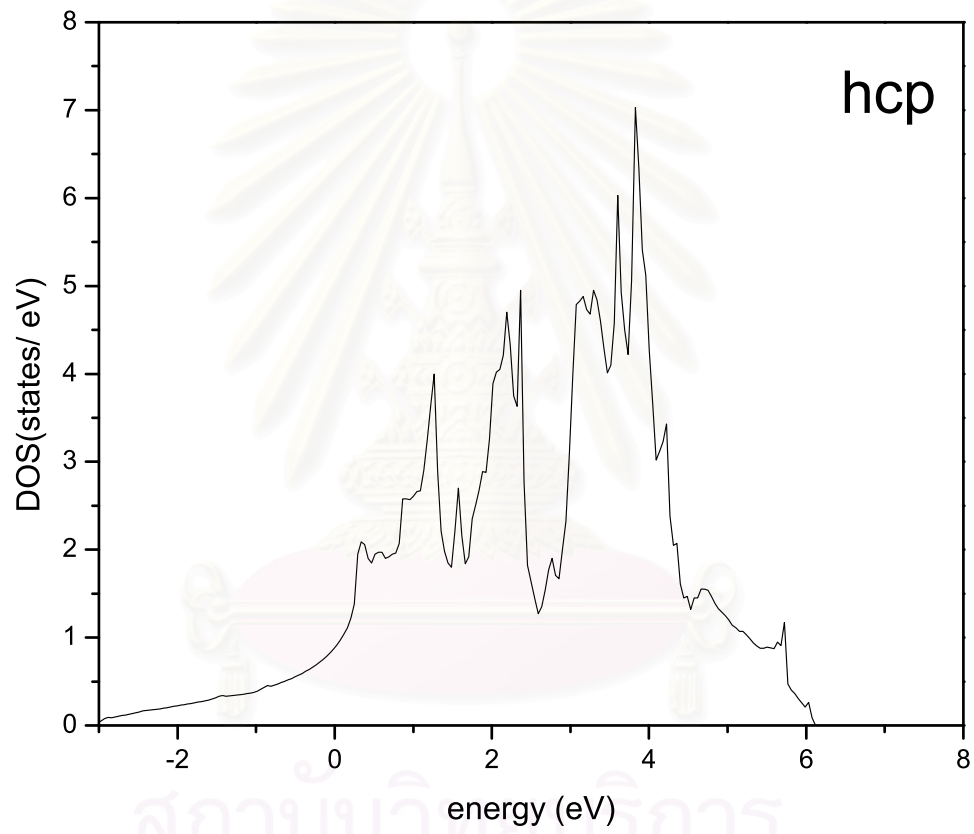


Figure 3.2: Electronic density of states for the hcp structures of Ti.[3]

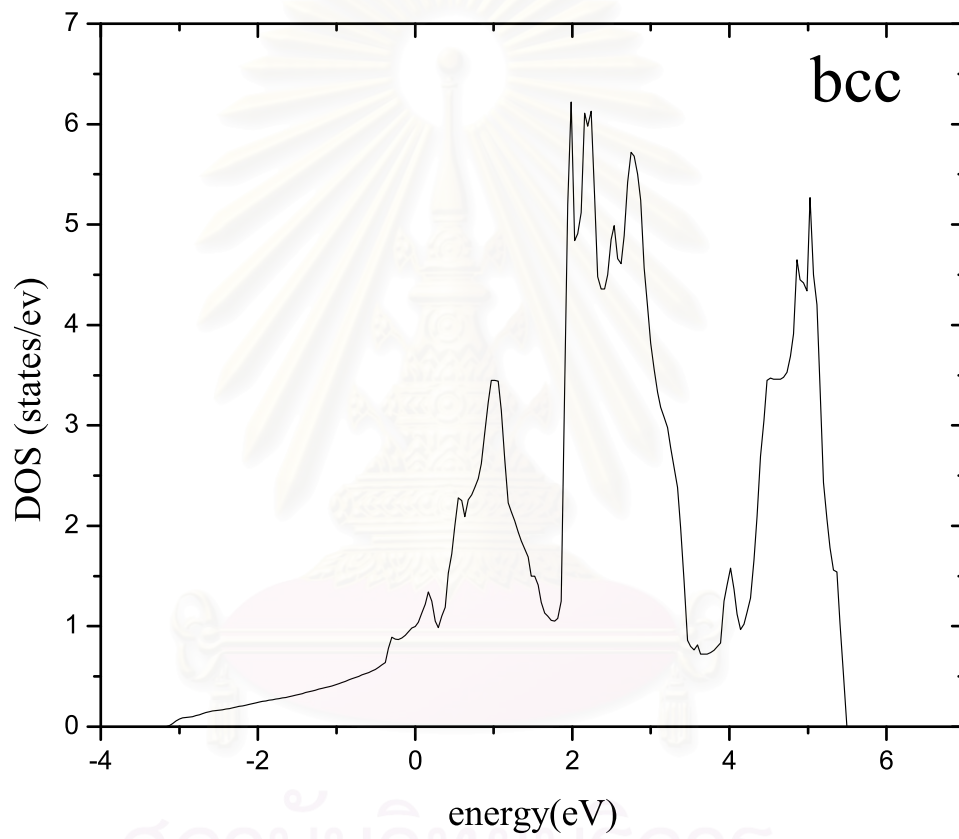


Figure 3.3: Electronic density of states for the bcc structures of Ti.[3]

# CHAPTER IV

## RESULTS AND DISCUSSION

In this chapter, we have applied molecular dynamics method to calculate the transition temperature ( $T_0$ ) of titanium. Helmholtz free energy  $A(T, V)$  is chosen for considering the phase transition. Helmholtz free energy is the state function of a system defined as.

$$A(T, V) = E(T, V) - TS(T, V). \quad (4.1)$$

where  $A(T, V)$  is Helmholtz free energy,  $E(T, V)$  is the internal energy of the system,  $T$  is the temperature, and  $S(T, V)$  is the total entropy. Under certain conditions of constant temperature and the constant volume, the change of Helmholtz free energy is useful in the prediction of the transformation of the states. The transformation of a system occurs at the state having the lowest Helmholtz free energy. For titanium, Helmholtz free energy difference  $\Delta A(T, V)$  between the bcc and the hcp phases is defined as

$$\Delta A(T, V) = A^{bcc}(T, V) - A^{hcp}(T, V). \quad (4.2)$$

where  $A^{bcc}$  is Helmholtz free energy of the bcc phase and  $A^{hcp}$  is Helmholtz free energy of the hcp phase. From Eq.(4.1) and Eq.(4.2), Helmholtz free energy dif-

ference can be written as

$$\Delta A(T, V) = \Delta E(T, V) - T\Delta S_{tot}(T, V), \quad (4.3)$$

where  $\Delta E(T, V)$  is the internal energy difference and  $\Delta S(T, V)$  is the total entropy difference. The both  $\Delta E(T, V)$  and  $\Delta S(T, V)$  components can be calculated from

$$\Delta E(T, V) = E^{bcc} - E^{hcp}, \quad (4.4)$$

and

$$\Delta S_{tot}(T, V) = S_{tot}^{bcc} - S_{tot}^{hcp}. \quad (4.5)$$

where  $S_{tot}^{hcp}$  and  $S_{tot}^{bcc}$  are the sums of the vibrational entropy and the electronic entropy of the hcp phase and the bcc phase respectively. Furthermore, Helmholtz free energy difference can be used to predict the phase transition, i.e.

$$\Delta A(T, V) \sim \begin{cases} > 0 \rightarrow A^{bcc} > A^{hcp}, & \text{the stable phase is the hcp phase.} \\ < 0 \rightarrow A^{bcc} < A^{hcp}, & \text{the stable phase is the bcc phase.} \\ = 0 \rightarrow A^{bcc} = A^{hcp}, & \text{the phase transition.} \end{cases}$$

In this work, we set the purpose to calculate the transition temperature. Thus, Helmholtz free energy for the both phases are calculated at constant volume  $V$  and constant temperature  $T$ . The internal energy difference and the difference of the product between the constant temperature and the total entropy will be

calculated at the following temperatures: 300K, 400K, 500K, 600K, 700K, 800K, 900K, 1,000K, 1,100K, 1,200K and 1,300K. The phase transition occurs at the transition temperature where  $\Delta A = 0$  or  $\Delta E = T\Delta S_{tot}$ .

In this chapter, we present the results of each component of Helmholtz free energy. First, the true lattice constant of the bcc and hcp phases are investigated and shown in Section (4.1). Second, the true lattice constant of each temperature, which includes the thermal expansion effects, is used to find the internal energy in Section (4.2). Next, the phonon density of states is presented in Section (4.3) and it is used for finding the vibrational entropy shown in Section (4.4). The electronic entropy is shown in Section (4.5). The finally, we calculate the transition temperature from Helmholtz free energy and it is shown in Section (4.6).

## 4.1 The True Lattice Constant

The purpose of this section is to calculate Helmholtz free energy of which a system kept at the constant temperature and the constant volume. In the simulation, we include the thermal energy arising from the temperature, and consider from the pressure. From Section 2.4, we determine the true lattice constant from the relation between the lattice constant and the pressure in molecular dynamics method.

For example, we obtain the pressure of the bcc phase which the lattice constant is assigned to  $a=3.2\text{\AA}$ ,  $3.25\text{\AA}$ ,  $3.28\text{\AA}$  and  $3.3\text{\AA}$  at  $T=1,100$  K from the **MD** simulations. It is illustrated in Fig.(4.1). The lattice constant and the average pressure are calculated and used to find the true lattice constant via linear fit of the data points. The true lattice constant is  $3.278\text{\AA}$  and will be used in the simulation for bcc phase at 1,100K.(It corresponds to the calculation of the hcp phase at 500K, Fig.2.5 (b) in Section 2.4.)

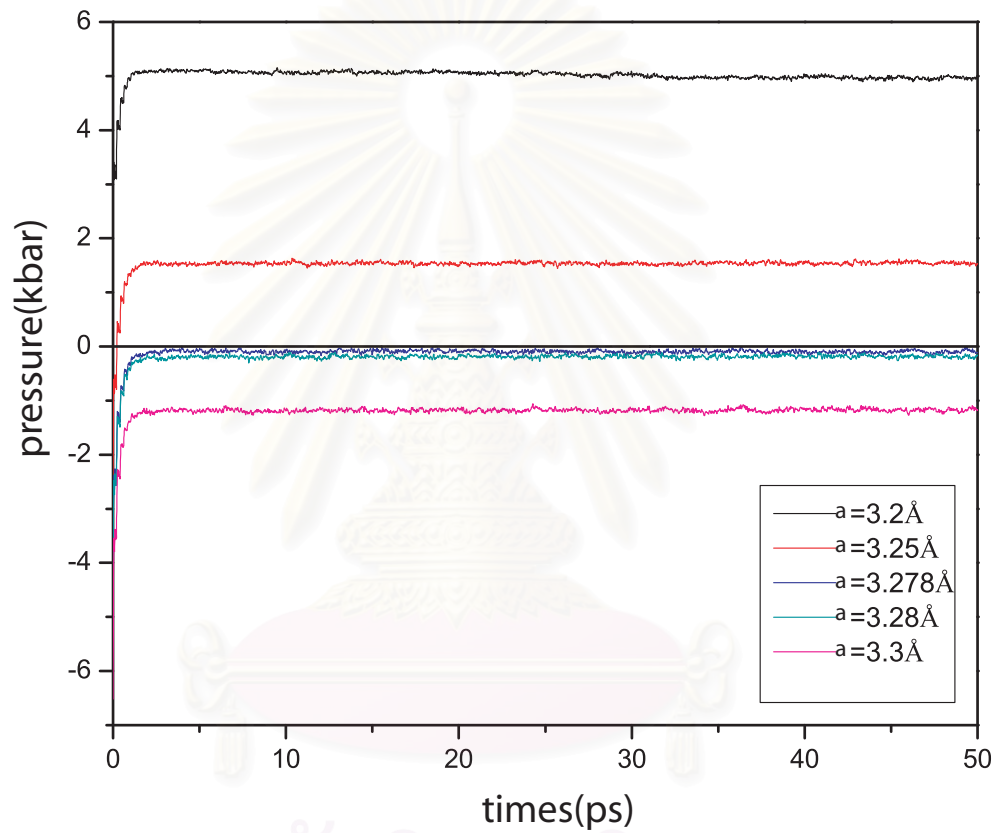


Figure 4.1: The pressure of the bcc phase for  $a=3.2\text{\AA}$ ,  $3.25\text{\AA}$ ,  $3.278\text{\AA}$ ,  $3.28\text{\AA}$  and  $3.3\text{\AA}$  at  $T=1,100K$ .



The lattice constant at  $P = 0$  for the bcc and hcp phases are calculated at temperature between  $300K$  to  $1,300K$ . The lattice constants of the bcc and hcp phases are shown in Fig.(4.2) and Fig.(4.3) respectively. The true volume at all temperature are used in MD simulations.

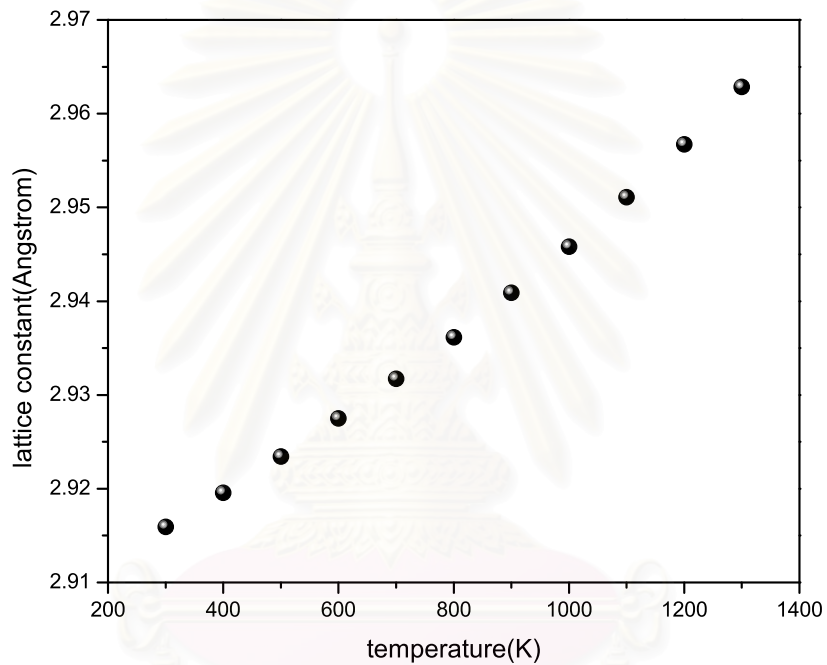


Figure 4.2: The lattice constant of the hcp phase with  $P=0$  at constant temperatures:  $T = 300K, 400K, 500K, 600K, 700K, 800K, 900K, 1,000K, 1,100K, 1,200K,$  and  $1,300K$

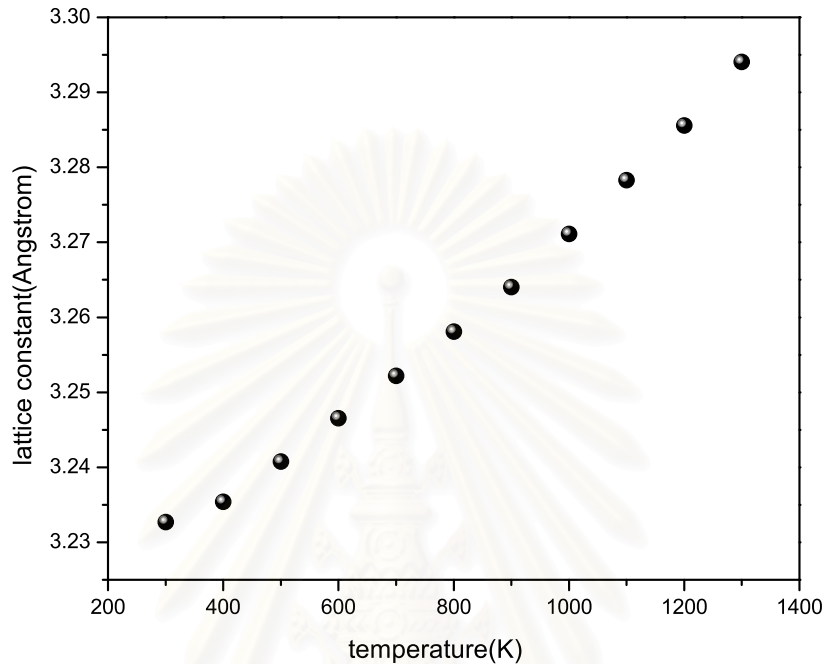


Figure 4.3: The lattice constant of the bcc phase with  $P=0$  at constant temperatures:  $T = 300K, 400K, 500K, 600K, 700K, 800K, 900K, 1,000K, 1,100K, 1,200K,$  and  $1,300K$

## 4.2 The Internal Energy Difference

The aim of this section is to calculate the internal energy difference ( $\Delta E$ ) in Eq.(4.4). The internal energy consists of the kinetic energy part and the potential energy part. We can calculate the internal energy difference from the potential energy difference at each constant temperature only. There is no contribution from the kinetic part because the kinetic energy per atom is  $\frac{3}{2}k_B T$  [19, 21, 23], depending on temperature. The kinetic energy of the bcc phase is equal to the

hcp phase at the same temperature. Thus, the kinetic terms of both phases cancel each other at every temperature. We determine only potential energy between the hcp and the bcc phases from the MD simulation.

The lattice constants of the hcp and the bcc phases from Fig.(4.2) and Fig.(4.3) are used to construct the simulation box at each constant temperature. The hcp simulation contains 6,912 atoms and the bcc simulation contains 8,192 atoms. We use the Finish-Sinclair type potential in Eq.(2.14) to find the potential energy. At the beginning, the system is in a non-equilibrium state. After a few picoseconds, the system approaches an equilibrium. The simulation results of the potential energy are shown in Fig.(2.2) and Fig.(2.3). The equilibrium values of potential energy of both phases are averaged at each temperature and shown in Fig.(4.4). The numerical values of the lattice constants and the potential energy are presented in Table 4.1. It is obvious that the hcp phase has lower potential energy for all range of temperature considered here. Using the energy alone, we can say that the hcp phase is stable. According to experiments, this is not true. It is found that after heating Ti samples to around 1,155K, it transforms from the hcp to the bcc structure. The explanation lies in the entropy part of Helmholtz free energy.

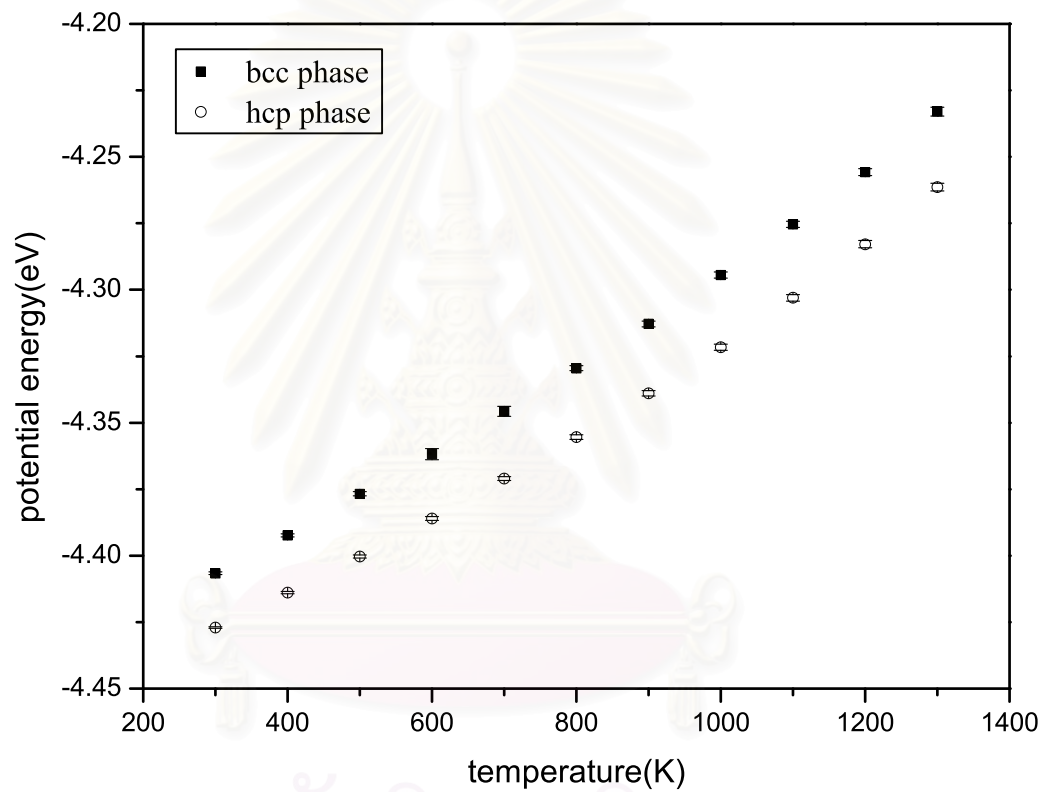


Figure 4.4: The potential energy of the hcp (open circles) and the bcc (filled squares) phases as a function of temperature.

$T(K)$	$a^{hcp}(\text{\AA})$	$a^{bcc}(\text{\AA})$	$E^{hcp}(eV)$	$E^{bcc}(eV)$
300	2.916	3.232	-4.427	-4.406
400	2.920	3.235	-4.414	-4.392
500	2.923	3.241	-4.400	-4.377
600	2.927	3.247	-4.386	-4.362
700	2.932	3.252	-4.371	-4.346
800	2.936	3.258	-4.355	-4.329
900	2.941	3.264	-4.339	-4.313
1000	2.946	3.271	-4.322	-4.294
1100	2.951	3.278	-4.303	-4.275
1200	2.957	3.286	-4.283	-4.255
1300	2.963	3.294	-4.261	-4.232

Table 4.1: Numerical figures of the potential energy ( $E$ ) and the lattice constants ( $a$ ) of the hcp and the bcc phases.

### 4.3 The Phonon Density of States

The phonon density of states (DOS) is the important part for calculating the vibrational entropy. The DOS can be derived from the MD simulation. We calculate the atomic velocity autocorrelation function,  $\gamma(t)$ , in Equation (3.22). The fourier transform of  $\gamma(t)$  gives directly the phonon density of states from Equation (3.18).

In our simulations, the time step between the origin to the end is  $10^{-12}$  sec. The VACF of the hcp phase is determined at temperature from 300 K to 1,300 K. The bcc phase is determined at 1,000K, 1,100K, 1,200K and 1,300K. The VACF of the bcc phase at the temperature lower than 1,000K can not be determined because the system undergoes from the bcc phase to the hcp phase in short interval. In Fig.(4.5), we show a typical velocity autocorrelation in the hcp phase at 300K, 400K and 500K, and the bcc phase at 1,000K, 1,100K and 1,200K in Fig.(4.6).

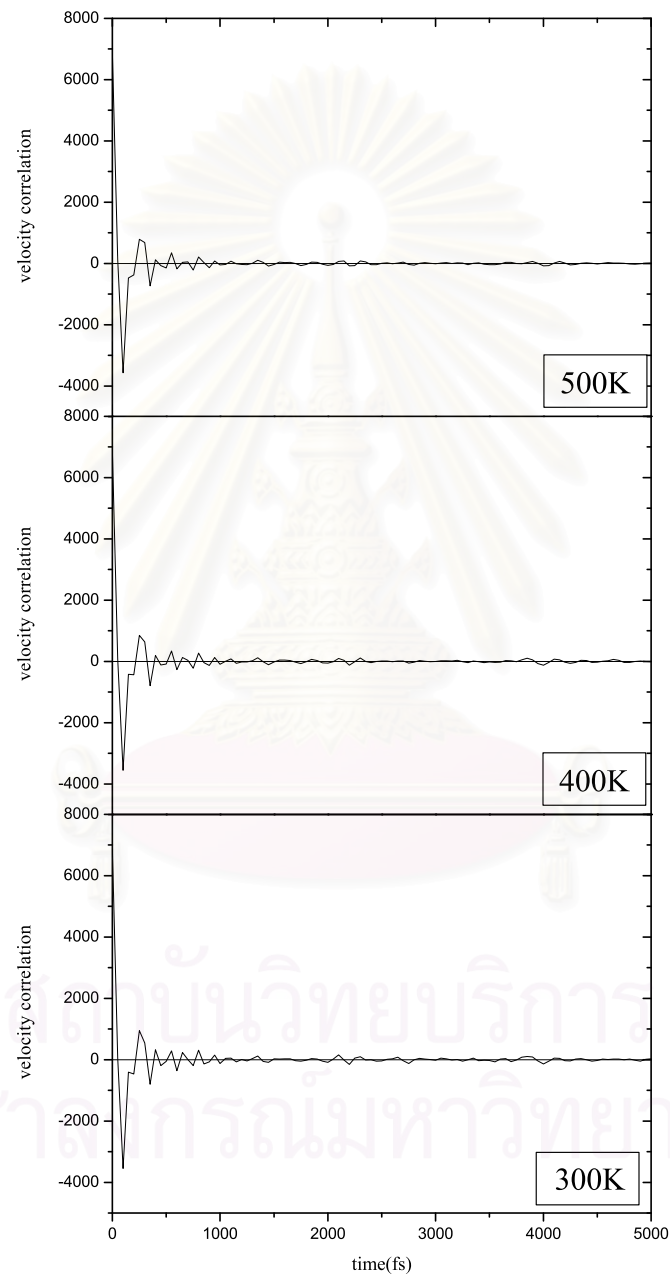


Figure 4.5: Velocity autocorrelation function of the hcp phase at 300K, 400K and 500K, going from bottom to top



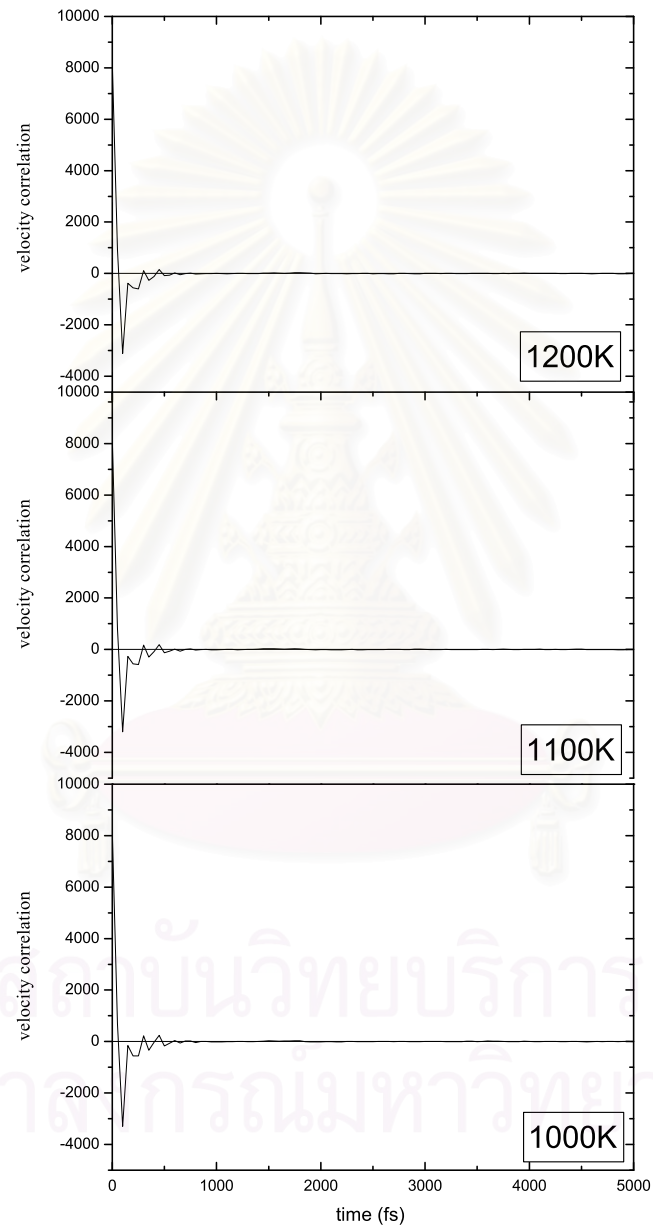


Figure 4.6: Velocity autocorrelation function of the bcc phase at 1000K, 1100K and 1200K, going from bottom to top

The Fourier transform of  $\gamma(t)$  gives directly the phonon density of states  $D(\omega)$ . The phonon density of states at 1,000 K for bcc and hcp phases are shown in Fig.(4.7) and Fig.(4.8) respectively as samples of the  $D(\omega)$ .

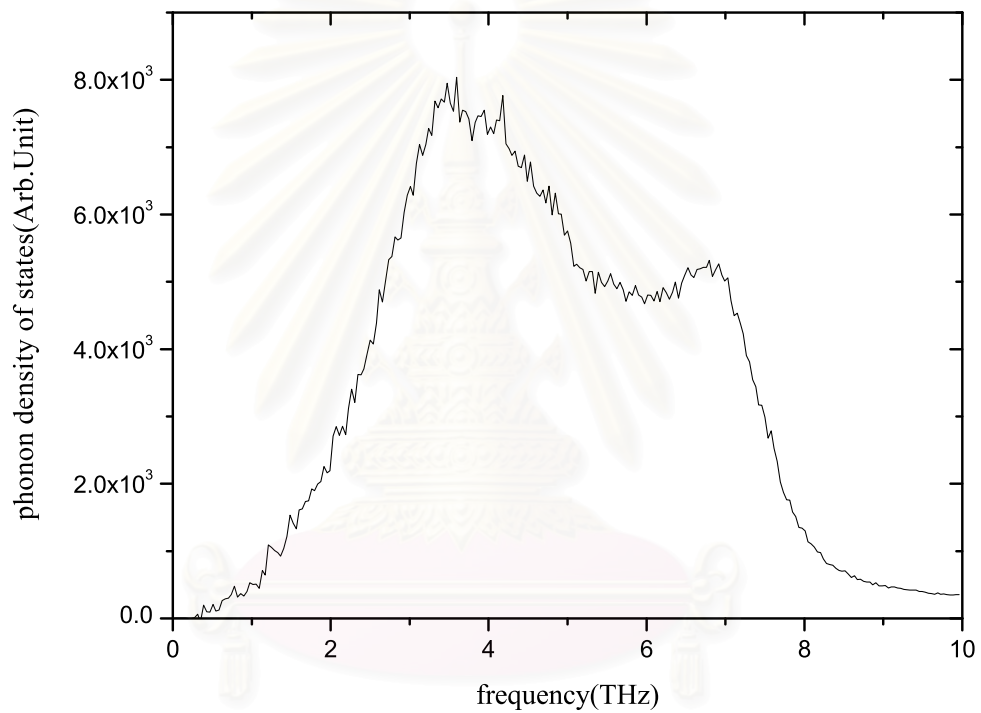


Figure 4.7: The phonon density of states of the hcp phase at 1,000K

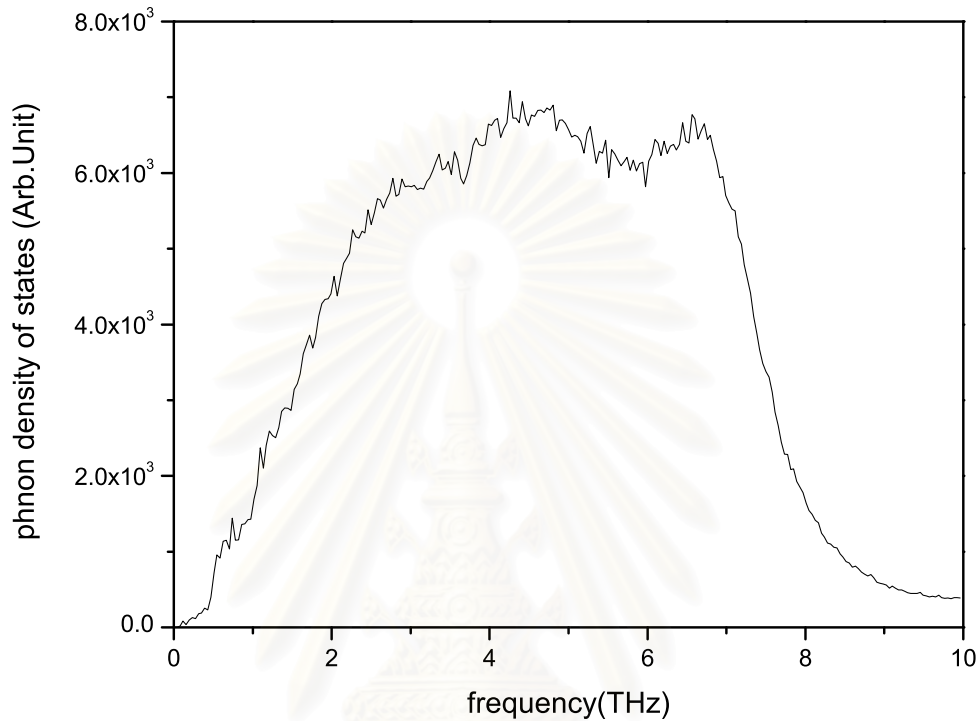


Figure 4.8: The phonon density of states of the bcc phase at 1,000K

#### 4.4 The Vibrational Entropy

The vibrational entropy is the entropy from the oscillations of the atoms. It contains the harmonic vibrational entropy and the anharmonic vibrational entropy. In this work, the harmonic vibrational entropy can be evaluated by Eq.(3.16). The harmonic vibrational entropy between the hcp phase and bcc phase as a function of temperature is shown in Fig.(4.9).

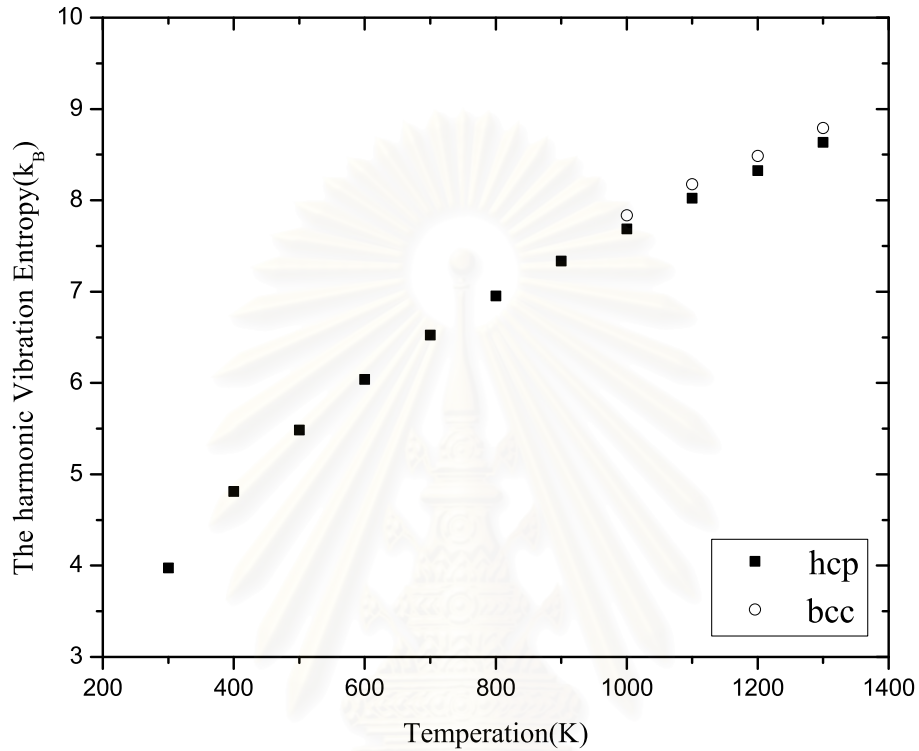


Figure 4.9: The calculated values of the harmonic vibrational entropy of the hcp (filled squares) and the bcc phases (open circles)

The harmonic vibrational entropy of the hcp phase is between  $3.9 k_B$  and  $8.7 k_B$  per atom from 300 K to 1,300 K and the bcc phase is between  $7.4 k_B$  and  $8.7 k_B$  per atom from 1,000 K to 1,300 K. The harmonic vibrational entropy of the bcc phase cannot determine at temperature lower than 1,000 K because the results in the MD simulations undergo a phase transition from the bcc phase to the hcp phase. We get a value of the harmonic vibrational entropy difference  $\Delta S_H = 0.15 k_B/atom$  at the phase transition temperature  $T_0 = 1,155 K$  from the interpolated values of the hcp phase and the bcc phase. It compared with the

experimental result is  $0.29k_B$ , reported by Petry et.al.[4]. The present  $\Delta S_H$  from MD is lower than experimental value. This is because the anharmonic effects are not included at high temperatures. So, we add the anharmonic part to improve the vibrational entropy. We extract the anharmonic contribution using a method suggested by Lacks and Shukla [25] in Eq.(4.10) at each temperature. The anharmonic vibrational entropy is shown in Fig.(4.10). Obviously, the anharmonic entropy in the bcc phase is three-to-four times larger than that of the hcp phase. This finding confirms that the excess entropy mostly comes from the anharmonic entropy.

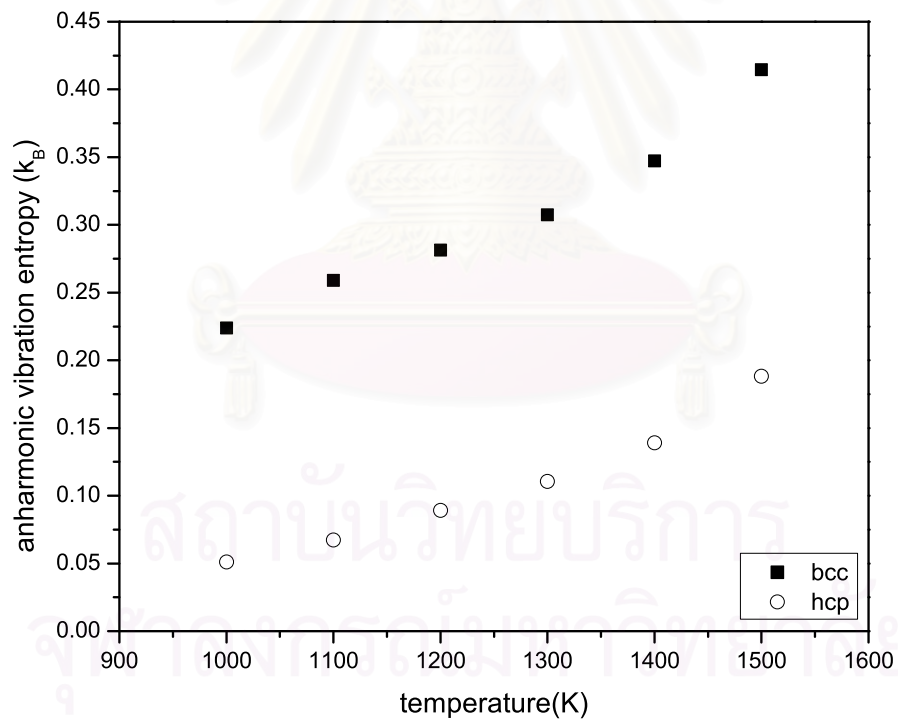


Figure 4.10: The anharmonic contribution of the hcp (open circles) and the bcc (filled squares) structures.

Consequently, we obtain the vibrational entropy from a summation of the harmonic vibrational entropy and the anharmonic vibrational entropy. The vibrational entropy in the hcp phase and the bcc phase are illustrated in Figures (4.11) and (4.12) respectively. The numerical values of the harmonic vibrational entropy and the anharmonic vibrational entropy are presented in Table 4.2. We observe that the vibrational entropy in the hcp phase is in a good agreement with experiments but the entropy in the bcc phase is higher than the experiments because the calculation of the anharmonic part from the **MD** has substantial values. Furthermore, we get a value of the total vibrational entropy difference  $\Delta S = 0.33 k_B$  per atom at transition temperature from the interpolation of the vibrational entropy in the bcc phase and the hcp phase. It is in a reasonable agreement with the experimental result [4]. This should confirm the accuracy of the model.



สถาบันวิทยบริการ  
จุฬาลงกรณ์มหาวิทยาลัย

$T(K)$	$S_H^{hcp}(k_B)$	$S_H^{bcc}(k_B)$	$S_A^{hcp}(k_B)$	$S_A^{bcc}(k_B)$
300	3.976	—	—	—
400	4.814	—	—	—
500	5.483	—	—	—
600	6.038	—	—	—
700	6.525	—	—	—
800	6.952	—	—	—
900	7.336	—	—	—
1000	7.689	7.837	0.051	0.224
1100	8.023	8.178	0.067	0.259
1200	8.327	8.485	0.089	0.282
1300	8.635	8.791	0.111	0.307

Table 4.2: Numerical figures of the harmonic vibrational entropy ( $S_H$ ) and the anharmonic vibrational entropy ( $S_A$ ) of the hcp and the bcc phases.



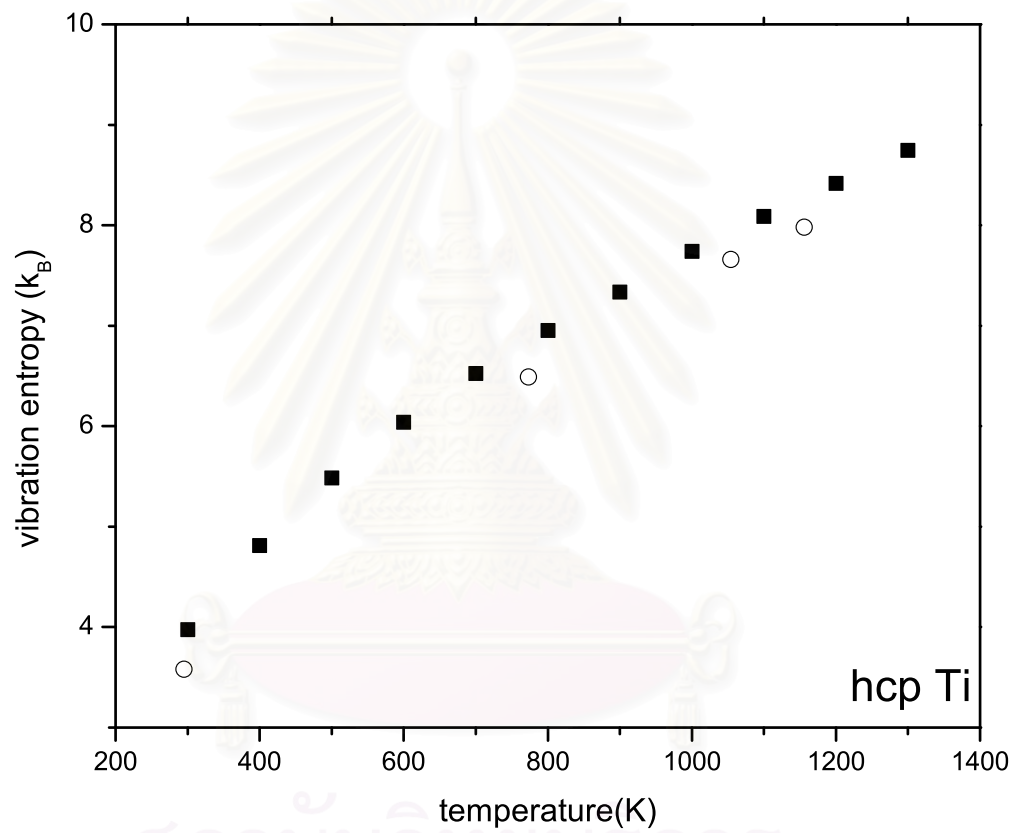


Figure 4.11: The calculated values of the total vibrational entropy of the hcp Ti (filled squares) compared with the experimental values [4] (open circles).

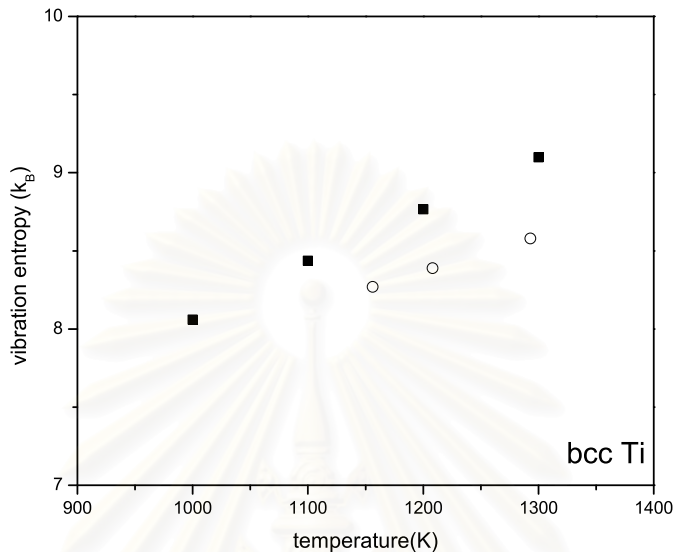


Figure 4.12: The calculated values of the total vibrational entropy of the bcc Ti (filled squares) compared with the experimental values [4] (open circles).

## 4.5 The Electronic Entropy

In this section, we present the values of the electronic entropy ( $S_E$ ). It is calculated from Eq.(3.35). We use the electronic densities of states from Ahuja, *et.al.*[3] which are calculated by a full potential linear muffin-tin orbital (FP-LMTO) in Fig.(3.2) for the hcp phase and Fig.(3.3) for the bcc phase. The electronic entropy of the hcp phase, the bcc phase and experimental values are graphed in Fig.(4.13) at each temperature. The numerical values of the electronic entropy are presented in Table 4.3. The magnitude of the electronic entropy of hcp is between  $0.16 k_B$  and  $0.93 k_B$  at  $T = 300\text{K} - 1,300\text{K}$  and between  $0.6 k_B$  and  $1.02 k_B$  for the bcc phase at  $T = 900\text{K} - 1,300\text{K}$ . Obviously, the agreement between experimental values and the calculated electronic entropy is good, particularly at low temperature.

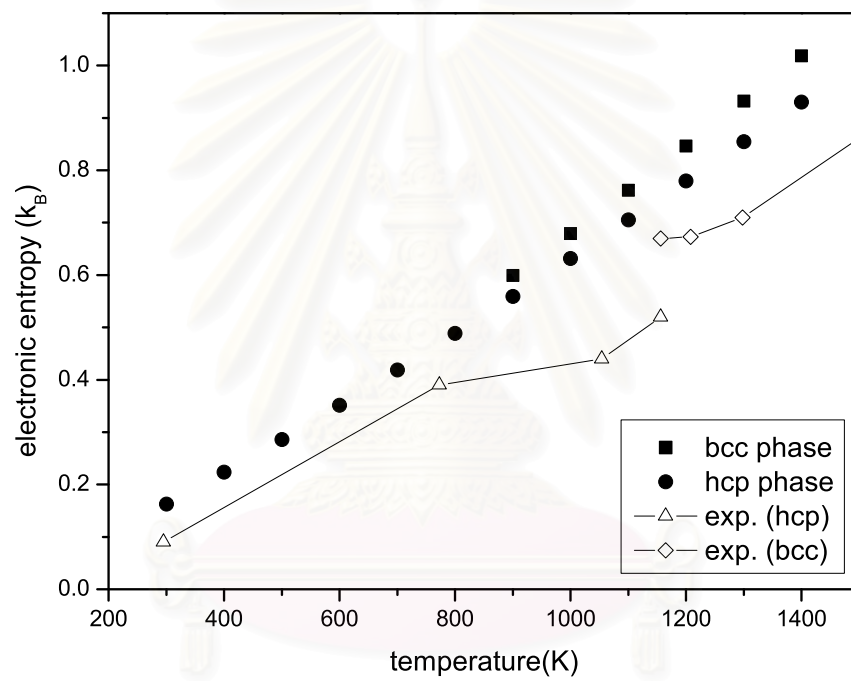


Figure 4.13: The electronic entropy of the hcp phase (circles), the bcc phase (squares) and the experimental values (open diamonds)[9].

$T(K)$	$S_E^{hcp}(k_B)$	$S_E^{bcc}(k_B)$	$T(K)$	$S_{E(exp.)}^{hcp}(k_B)$	$S_{E(exp.)}^{bcc}(k_B)$
300	0.163	—	-	—	—
400	0.223	—	-	—	—
500	0.286	—	294	0.09	—
600	0.352	—	773	0.39	—
700	0.419	—	1054	0.44	—
800	0.48	—	1156	0.52	—
900	0.559	0.599	1156	—	0.670
1000	0.632	0.679	1208	—	0.673
1100	0.705	0.762	1298	—	0.710
1200	0.780	0.847	1538	—	0.890
1300	0.855	0.932	1713	—	0.990

Table 4.3: Numerical figures of the electronic entropy ( $S_E$ ) from MD method and experimental values [9] of the hcp and the bcc phases.

## 4.6 The Transition Temperature

In our work to the calculation of the transition temperature ( $T_0$ ) for Ti, we use Helmholtz free energy difference ( $\Delta A$ ) to find the hcp-bcc phase transition and  $T_0$ . It is defined as  $\Delta A = \Delta E - T\Delta S_{tot}$ , where  $\Delta S_{tot} = S_{tot}^{bcc} - S_{tot}^{hcp}$ . The phase transition occurs at  $T_0$  where  $\Delta A = 0$ . The values of  $\Delta E$  are estimated in Section 4.2 and those of  $S_{tot}^{hcp}$  and  $S_{tot}^{bcc}$  are calculated by using a summation of the vibrational entropy in Section 4.4 and the electronic entropy in Section 4.5. Figure 4.14 shows  $\Delta E$  (filled square) and  $T\Delta S_{tot}$  (open circles) as a function of temperature.

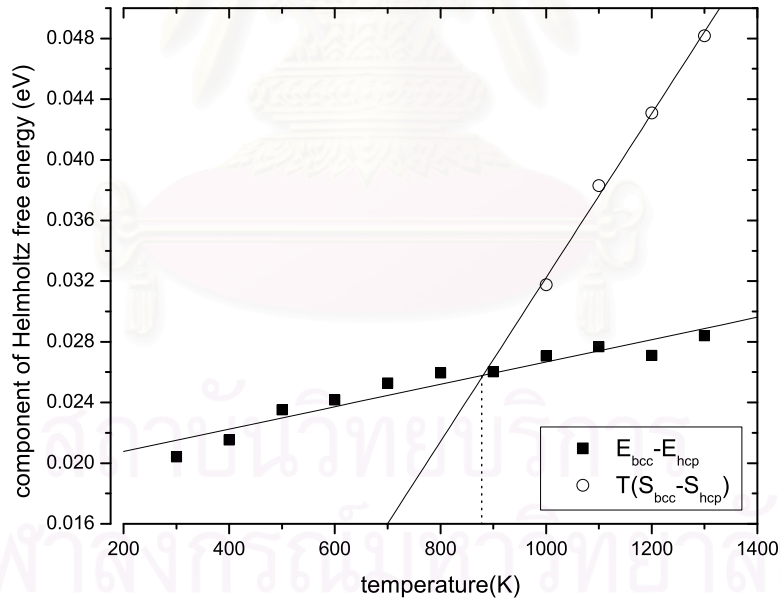


Figure 4.14: The components  $\Delta E$  (filled square) and  $T\Delta S$  (open circles) of the Helmholtz free energy.

From Fig.(4.14), linear fits are applied to  $T\Delta S$  and  $\Delta E$ . By using the analytical process, the intersection between  $\Delta E$  and  $T\Delta S$  occurs at  $880K$ . Thus, the transition temperature is  $880K$  where  $\Delta A=0$ . Moreover, we predict the stable phase at other temperatures. If  $T < 880$ , the stable phase is the hcp phase because  $A_{hcp} < A_{bcc}$ . If  $T > 880K$ , the stable phase is the bcc phase  $A_{bcc} < A_{hcp}$ . The transition temperature from our work is  $880K$  compared with some previous calculations such as ,  $3,350K$  by Craievich [7],  $2,050K$  by Moroni [6], and with  $1,155K$  from experimental results . Hence our calculations are in good agreement with experiments and yet better than those of some previous works because our results included the anharmonic vibrational entropy effects and the electronic entropy effects in the free energy difference.

In addition, we observed that our result is  $T_0 \approx 880K$  calculated with the thermal electronic contributions. On the other hand, our previous result [33] is evaluated at  $T_0 \approx 906K$  calculated without the thermal electronic contributions. It seems that our previous result is in better agreement with experiments than the present result including the contributions of thermal electronic. However, this is not conclusive because the error from the calculations has not been evaluated. A previous MD work suggested that the error of the transition temperature in similar transition metals [1, 24], is about  $\pm 200K$ . Including such an error, we can see that  $880K$  and  $906K$  are not significantly different. Thus, we conclude that the electronic entropy is a minor contribution in determining the phase transition and the electronic entropy difference is  $0.06k_B$  at transition temperature. This is confirmed by an independent work. Recently, Masuda-Jindo, *et.al.*[10] calculated transition temperature of Ti using the statistical moment method. They found that transition temperatures are  $1,295K$  and  $1,308K$  which are calculated with and without the thermal electronic contributions respectively.

# CHAPTER V

## CONCLUSIONS

The purpose of this thesis is to determine the transition temperature ( $T_0$ ) of titanium. From experimental values, the phase transition occurs at high temperature,  $T_0 = 1,155K$ . We use computer simulation to study the bcc-hcp phase transition. In this work, we consider the Helmholtz free energy ( $A$ ) at constant temperature and constant volume. At thermodynamics equilibrium, the stable phase has the lowest Helmholtz free energy. The Helmholtz free energy difference ( $\Delta A$ ) between bcc phase and hcp phase is defined,  $\Delta A = \Delta E - T\Delta S$ . The internal energy difference ( $\Delta E$ ) and total entropy difference ( $\Delta S$ ) need to be calculated at various temperatures.

In this work, classical molecular dynamics method (MD) is employed to determine the vibrational entropy and the potential energy. The MD is simulated under constant temperature and constant volume. In our simulations, we set the structure to be either the bcc or hcp at the starting-time. The Finnis-Sinclair potential energy is chosen to represent the potential energy of titanium because it takes into account of many-body effects and gives a good description for both hcp and bcc phases. The motions of atoms are solved by Newton 's equations. We choose Gear Predictor Corrector method for integrating the equations of motion.

From the MD simulations, we obtain the potential energy and velocity of each atom of the bcc and hcp phases at every time step. The internal energy



difference can be calculated from the potential energy difference because the kinetic energy of both phases at the same temperature cancels. Obviously, the hcp phase has lower potential energy than bcc phase for all range of temperatures considered. If we consider the potential energy only, the stable phase is the hcp phase which is not true. We know that Ti has a phase transition from hcp to bcc at high temperatures. So the entropy part should play a major role in the phase transition.

The total entropy [9] consists of the harmonic vibrational entropy ( $S_H$ ), the anharmonic vibrational entropy ( $S_A$ ) and the electronic entropy ( $S_E$ ). The harmonic vibrational entropy is derived from the phonon density of states which is calculated via the fourier transform of the velocity autocorrelation function (VACF). The VACF is evaluated from the velocity of each atom. The anharmonic vibrational entropy is computed from the anharmonic free energy. We assume that the summation of  $S_H$  and  $S_A$  is the total vibrational entropy. We find that  $\Delta S_{vib} \approx 0.33 k_B/\text{atom}$  at transition temperature,  $T = 1,155K$ . It can be compared with  $\Delta S_{vib} \approx 0.29 k_B/\text{atom}$  from the experiment [4]. Our result is in an agreement with the experimental value. The electronic entropy is calculated from the electronic density of states which is obtained from Ahuja, *et. al.*[3]. The magnitude of the electronic entropy of hcp is between  $0.16 k_B$  and  $0.93 k_B$  at  $T = 300K - 1,300K$  and between  $0.60 k_B$  and  $1.02 k_B$  for the bcc phase at  $T = 900K - 1,300K$ .

We evaluated  $\Delta E$  and  $T\Delta S$  at  $300K$  to  $1,300K$ . Linear fits are applied to  $\Delta E$  and  $T\Delta S$ . The transition temperature occurs at the intersection between  $\Delta E$  and  $T\Delta S$ ,  $T_0 \approx 880K$ . It can be compared with  $1,155K$  from experiment,  $3,350K$  by Craievich [7],  $2,050K$  by Moroni [6],  $1,308K$  and  $1,295K$  by Masude-Jindo [10]. We found that our result is in an agreement with the experiment and the transition temperature is better than the previous report since the anharmonicity effects of thermal lattice vibrations are included in this research. In addition,

our results can be compared with our previous results [33] which are calculated without the thermal electronic contributions. It is showed that both values differ minimally. We conclude that the MD method is a good computational method for studying the phase transition in Ti and the calculation of transition temperature in Ti is not affected much by the electronic entropy. In addition, we found that the MD method is nowadays also used for other purposes such as studies of the anharmonic contribution for a fcc crystal of atoms interacting via Lennard-Jones potential [25], thermal conductivity of solid argon [34], the density as a function of pressure for the crystal structure of Ne, Ar, Kr, and Xe [35] and the transition temperature of zirconium [2, 24, 26].



สถาบันวิทยบริการ  
จุฬาลงกรณ์มหาวิทยาลัย

# REFERENCES

1. Srepusharawoot, P. *The phase transition temperature int Zirconium metal from the classical molecular dynamics method*. Master's thesis, Faculty of Science, Chulalongkorn University, (2003).
2. Pinsook, U. *Computer simulations of martensitic transition in zirconium*. Ph. D. thesis, The University of Edinburgh, (1999).
3. Ahuja, R., Wills, J.M., Johansson, B., and Eriksson, O. Crystal structures of Ti, Zr, and Hf under compression: Theory. *Phys. Rev. B* **48** (1993): 16269.
4. Petry, W., Heiming, A., Alba, M., Heraig, C., Schober, H.R., and Vogl, G. Phonon dispersion of the bcc phase of group-IV metals. I. bcc Titanium. *Phys. Rev. B* **43** (1991): 10933.
5. Ye, Y.-Y., Chen, Y., Ho, K.M., Harmon, B.N., and Lindgård, P.-A. Phonon-Phonon Coupling and the Stability of the High-Temperature bcc Phase of Zr. *Phys. Rev. Lett.* **58** (1987): 1769.
6. Moroni, E.G., Grimvall, G., and Jarlborg, T. Free energy contributions to the hcp-bcc transformation in transition metals. *Phys. Rev. Lett.* **76** (1995): 2758.
7. Craievich, P.J., Sanchez, J.M., Watsom, R.E., and Weinert, M. Structural instabilities of excited phases. *Phys. Rev. B* **55** (1997): 787.
8. Heiming, A., Petry, W., Trampenau, J., Alba, M., Herzig, C., Schober, H.R., and Vogl, G. Phonon dispersion of the bcc phase of group-IV metals.

- II. bcc zirconium, a model case of dynamical precursors of martensitic transitions. *Phys. Rev. B* **43** (1991): 10948.
9. Eriksson, O., Wills, J.M., and Wallace, D. Electronic, quasiharmonic, and anharmonic entropies of transition metals. *Phys. Rev. B* **46** (1992): 5221.
  10. Masuda-Jindo, K., Nishitani, S.R., and Hung, V.V. HCP-BCC Structural phase transformation of Titanium. *Phys. Rev. B* **70** (2004): 184122-1.
  11. Ackland, G.J. Theoretical study of titanium surfaces and defects with a new many-body potential. *Phil. Mag. A* **66** (1992): 917.
  12. Press, W.H., Flannery, B.P., Teukolsky, S.A. and Vetterling, W.T. *Numerical Recipes in C: The Art of Scientific Computing*. Cambridge: Cambridge University Press, (1986).
  13. Gear, C.W. *Numerical Initial Value Problems in Ordinary Differential Equations*. New Jersey: Prentice-Hall, (1971).
  14. Ackland, G.J., Tichy, G.I., Vitek, V., and Finnis, M.W. Simple N-body potentials for the noble metals and nickel. *Phil. Mag. A* **56** (1987): 735.
  15. Ackland, G.J. *Non-Pairwise potentials and defect modelling for transition metals*. Ph. D. thesis, Oxford University, (1987).
  16. Srepusharawoot, P., and Pinsook, U. The BCC-HCP Transition Temperature in Zirconium. *J. Sci. Res. Chula. Univ* **27** (2002): 131.
  17. Trampenau, J., Petry, W., Heiming, A., Alba, M., Heraig, C., and Schober, H.R. Phonon dispersion of the bcc phase of group-IV metals III. bcc hafnium. *Phys. Rev. B* **43** (1991): 10963.

18. Ercolessi, F. *A Molecular Dynamics Primer* Trieste: Spring college in computational physics, (1997).
19. Amit, D.J., and Verbin, V. *Statistical Physics: An Introductory Course*. Singapore: World Scientific, (1999).
20. Kittel, C. *Introduction to Solid State Physics*. New York: John Wiley & Sons, (1986).
21. Huang, K. *Statistical Mechanics*. Canada: John Wiley & Sons, (1987).
22. Dickey, J.M., and Paskin, A. Computer simulation of the lattice dynamics of solids *Phys. Rev. B* **188** (1969): 1407.
23. Mandl, F., *Statistical Physics*. Great Britain: John Wiley & Sons, (1988).
24. Srepusharawoot, P., and Pinsook, U. Application of entropy calculations to the determination of transition temperature in Zirconium. *Phys. Stat. Sol (b)* **242** (2005): 1598-1605.
25. Lacks, D.J., and Shukla, R.C. Molecular dynamics and higher-order perturbation-theory results for the anharmonic free energy and equation of state of a Lennard-Jones solid. *Phys. Rev. B* **54** (1996): 3266.
26. Pinsook, U. Molecular dynamics of study of vibrational entropy in bcc and hcp zirconium. *Phys. Rev. B* **66** (2002): 24109.
27. Nishitani, S., Kawabe, H., and Aoki, M. First-principle calculations on bcc-hcp transition of titanium. *Materials Science and engineering* **A312** (2001): 77-83.
28. Willaime, F. and Massobrio, C. Development of an N-body interatomic potential for hcp and bcc zirconium. *Phys. Rev. B* **43** (1990): 11653.

29. Hygh, E.H., and Welch, R.M. Electronic structure of Titanium. *Phys. Rev. B* **1** (1969): 2424.
30. Welch, R.M., and Hygh, E.H. Electronic structure of Titanium III. *Phys. Rev. B* **9** (1973): 1993.
31. Paxton, A.T. Structural energy-volume relations in first-row transition metals. *Phys. Rev. B* **41** (1989): 8127.
32. Hultgren, R., Desai, R.D., Hawkins, D.T., Gleiser, M., Kelley, K.K., and Wagman, D.D. *Selected Values of the thermodynamics Properties of the Elements*. Metal Park, Ohio: American Society for Metals, (1973).
33. Chureemart, J., and Pinsook, U. The transition temperature of the hcp-bcc phase transition in Titanium. *J. Sci. Res. Chula. Univ.* **31** (2006).
34. Konstantin, V.T., and Sandro, S. Thermal conductivity of solid argon from molecular dynamics simulations. *J. Chem. Phys.* **120** (2003): 3765.
35. Raffaele, G.D.V., and Elisabetta, V. Quasiharmonic lattice-dynamics and molecular-dynamics calculations for the Lennard-Jones solids. *Phys. Rev. B* **58** (1997): 206.



# VITAE

Mr. Jessada Chureemart was born on May 18, 1980 in Nakhon Phanom. He received his bachelor degree of Science in Physics from Khonkaen University in 2001 and obtained scholarship from the Development and Promotion of Science and Technology Talents Project (DPST) during his study.

## Conference Presentations:

- 2004 J. Chureemart, P. Srepusharawoot and U. Pinsook. The BCC - HCP Transition Temperature in Titanium and Zirconium metals using the Classical Molecular Dynamics Method. *4th National Symposium on Graduate Research*, Lotus Hotel Pang Suan Kaew, Chiangmai (10-11 August 2004): O-ST-55
- 2005 J. Chureemart and U. Pinsook. The BCC - HCP Transition Temperature in Titanium metal. *5th National Symposium on Graduate Research*, The Kasetsart University, Bangkok (10-11 October 2005): O-ST-80
- 2005 J. Chureemart and U. Pinsook. The analysis of the BCC-HCP transition temperature in Titanium metal *31<sup>th</sup> Congress on Science and Technology of Thailand*, The Suranaree University of Technology, Nakhon Ratchasima (18-20 October 2005): D 0035

## Research Publication:

- 2006 J. Chureemart and U. Pinsook. The transition Temperature of the hcp-bcc phase transition in Titanium. *Journal of Scientific Research Chulalongkorn University* 31 (2006)